Università degli Studi di Catania

SCUOLA SUPERIORE di CATANIA
MEDITERRANEAN UNIVERSITY CENTER

Università degli Studi di Catania
Scuola Superiore di Catania

International PhD

in

STEM CELLS

XXIV cycle

Exploring Cancer Stem Cells (CSCs) pathways to design novel therapies for glioblastoma treatment

Simona di Martino

Coordinator of PhD

Prof.……

Tutor

Prof. ……..……..

a.a. 2009/2011

Index

Abstract

Glioblastoma multiforme (GBM) is the most aggressive and common form of primary brain tumor in adults, with a median survival rate of 14 months (Taphoorn et al.;2005). GBM is characterized by rapid diffusely infiltrative growth and high level of cellular heterogeneity, which are fueled by dysregulation of multiple signaling pathaways. It is also characterized by multiple genetic alterations: the most frequent is the loss of heterozygosity (LOH) 10q; there are also epidermal growth factor receptor (EGFR) amplifications, TP53 and phosphatase and tensin homolog (PTEN) mutations. GBM is classified into primary glioblastoma developing rapidly *de novo* and secondary glioblastoma, usually developing from lower grade astrocytomas. Despite major therapeutic improvements made by combining neurosurgery, radiotherapy and chemotherapy, the prognosis and survival rate for patients with GBM remains poor (A.F.Carpentier and J.Y. Delattre. ;2005). There is a recognized need for new approaches based on increased understanding of the biological and molecular nature of these tumors.

In recent years, it has been demonstrated that GBM possesses a hierarchical organization of heterogeneous cell populations which differ in their tumor-forming potential: there are both cells with a limited lifespan that are destined to abortive differentiation and will eventually stop dividing, and a small subset of self-renewing tumoral cells capable of initiating and maintaining tumor growth. These cells are called Glioblastoma Stem Cells (GBM-SCs) and share several features with neural stem cells (NSCs) including: the expression of neural markers such as Nestin and Sox2, the ability to migrate within the brain, the capacity to self-renew and to undergo multilineage differentiation and the responsiveness to similar signalling cues. Moreover, when compared to their non-stem progeny, GBM-SCs also show increased resistance to drugs and to the apoptosis-inducing mechanisms that are effective in conventional tumoral cell lines. The isolation of GBM-SCs has introduced a new and revolutionary paradigm in cancer therapy, since these cells are likely to include a population able to support tumor relapse and should therefore be considered a primary therapeutic target (Hirschmann-Jax, C. et al.;2004, Dean, Fojo, & Bates; 2005).

Current therapeutic strategies do not take into account potential differences in drug sensitivity between the tumorigenic and the more abundant non-tumorigenic cells in the tumor. The opportunity to study GBM-SCs adds a radical change to the perspective by which the neoplastic phenomenon is observed and prompts for a detailed analysis of the molecular determinants of

tumorigenicity. Indeed it has been suggested that tumor relapse after conventional chemotherapeutic treatment might be a consequence of an expansion sustained by Cancer Stem Cells (CSCs) that are spared by virtue of their relative quiescence and the expression of drug-effluxing membrane transporters. In this project, we proposed to identify therapeutic agents that efficiently kill GBM-SCs and might be useful to set up more effective treatments for GBM . To this aim, we analyzed the expression profiling of microRNAs (miRNAs) in samples in order to identify those with potential importance in tumor biology and we performed *in vitro* citotoxicity assays on our GBM-SC lines using a library of 80 kinase inhibitors, in order to identify and target pathways involved in tumor progression and maintenance.

MiRNAs are emerging as important regulators of many biological processes, such as cellular differentiation and proliferation and have been implicated in the etiology of a variety of cancer. Libraries of synthetic compounds with known specificity have been screened *in-vitro* with the aim to study the sensitivity of tumor cells to the inhibition of a specific signal transduction pathway and the consequent development of targeted therapies.

Introduction

Glioblastoma Multiforme

Glioblastoma Multiforme (GBM) is the most common and aggressive tumors derived from glial cells and include tumors of astrocytic, oligodendrial, ependymal, or mixed origin. The standard name for this brain tumor, as defined by yhe World Health Organization (WHO), is glioblastoma. The term was coined by Mallory in 1914 and consolidated in the lexicon of surgery by Bailey and Cushing neuropathology in 1926. The designation "multiforme" suggests that the GBM shows marked intratumor heterogeneity on the cytopathological, transcriptional and genomic levels (Miller & Perry, 2007). In other words, the cellular composition can considerably vary and histological features of mixed type typical. This complexity, combined with the hypothesis of the existence of a subpopulation of cancer stem cells and an incomplete injury (epi) genetic basis , has made GBM one of the most complex to understand and treat cancer (Frank. et al ., 2008).

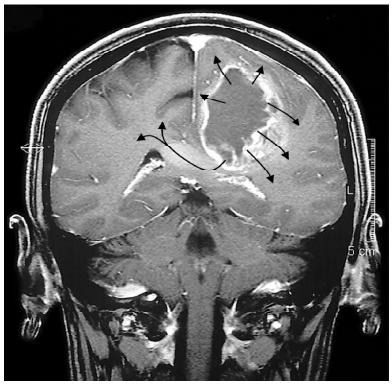

Figure 1.Image obtained by magnetic resonance imaging of a glioblastoma in the left side of the brain. The tumor presented active infiltration into the surrounding areas including the corpus callosum, the arrows indicate the directions of the tumor infiltrative fronte.

Epidemiologic Features

Glioblastoma multiforme may present at any age, but typically affects adults, with increasing incidence until aged 85 and above. The median age at diagnosis is 64 years, with more than 80 % of diagnosed GBM patients being older than 55 years and only 1 % younger than 20 years. Males are more commonly affected, with an incidence rate almost 1.6 times higher than in females. The glioma incidence is generally higher in the Western world com-pared to less developed countries (Curado, Edwards, Shin, et al.,2007). The major reason of the higher glioma incidence in developing countries is currently under ascertainment but is related to limited access to health care, variations in diagnostic practices, and incomplete reporting of glioma cases (Fisher., et al 2007). Moreover, some reports also indicate that ethnic differences in glioma susceptibility may exist. For example, in the United States GBM is more frequent in Caucasians than in people of African and Asian descent. A 1-2 % annual increase in the total brain tumor incidence occurred through the 1980s and 1990s, which pri-marily is thought to reflect the improved clinical diagnosis of neurological diseases after introduction of high-resolution neuroimaging in the early 1980s. However, a true rise in incidence for at least some types of brain tumors cannot be excluded, but such evidence are yet to be demonstrated for GBM.

For the majority of gliomas no underlying carcinogenetic causes can be identified. So far, the only established environmental risk factor reported is exposure to high-dose, ionizing radiation

(Il' yasova, et al., 2008). Several epidemiological studies have also demonstrated an association between increased glioma risk and other environmental factors, including severe head injury, dietary risk factors, occupational risk factors, and exposure to electromagnetic fields. However, the data regarding the suggested risk factors remain inconclusive, since other studies failed to identify any link to glioma development. (Wiemels., et al., 2007 and Berger., et al 2002). More consistent reports suggest a protective effect of allergic diseases and infections, indicating that immune surveillance mechanisms stimulated by these conditions, inhibit glioma development .
Genetic predisposition has been observed in 5-10 % of glioma cases (Wiemels., et al., 2007). Rare genetic syndromes associated with an increased risk of glioma such as neurofibromatosis 1 and 2, tuberous scle-rosis, retinoblastoma (RB) 1, Li-Fraumeni syndrome, Turcot's syndrome, and multiple harmatoma only account for few cases. Gliomas have also been observed to run in families, not affected by the listed syndromes, but implicated susceptibility genes remains yet to be identified. In addition, the causal relationship between glioma and common polymorphisms in genes involved in detoxification of carcinogens, cell cycle regulation, and DNA repair mechanisms, have been investigated only to reveal vague or no association. (Wiemels., et al., 2007 and Il' yasova, et al., 2008)

Pathological Features

Glioblastoma multiforme lesions are typical large at the time of diagnosis and may occupy much of a brain lobe. The lesions are often located in the subcortical white matter of the cerebral hemispheres and frequently extend across the border of the frontal lobe into the temporal lobe. Tumor infiltration has often progressed into the adjacent cortex and through the corpus callosum into the contralateral hemisphere. (Cavenee., et al., 2007).
The tumor mass of GBM is characterized by being poorly delineated and having a high degree of regional heterogeneity. Highly proliferating cancer cells are usually found in the peripheral, hypercellular zone of the tumor, whereas the central tumor area mainly consists of necrotic tissue, comprising up to 80 % of the total tumor mass. Histopathologically, the lesions typically exhibit cellular hyperplasia in peripheral zones harboring cancer cells with atypical nuclei, in-creased mitotic activity, cellular pleomorphism and poor stages of differentiation. A diagnostic feature of GBM is the presence of areas with vascular hyperplasia, necrosis or both in the tumor tissue. Another hallmark of GBM is rapid invasion of the surrounding brain tissue,

especially along myelinated brain structures such as the corpus callosum or within perivascular spaces. Infiltrating tumor cells are dispersed within the normal brain tissue surrounding the contrast-enhancing tumor border at high-resolution scans. These satellite cancer cells are thought to be the origin of local tumor recurrence after therapy, since the infiltrating cells escape surgical resection and high-dose radiotherapy of the primary tumor mass. Despite the highly infiltrative nature of GBM, it does not tend to invade neither the subarachnoidal space nor the vessel lumen, and therefore distant metastases are rarely found, both within and outside the Central Nervous System (CNS). (Cavenee., et al., 2007).

GBM lesions most commonly occur as primary GBM a without clinical evidence of a preceding lesion within the CNS (Ohgaki, Kleihues., 2007 and Stegh., et al ., 2007). Only about 5 % of GBM cases progress from lower grade astrocytomas into secondary GBM (Ohgaki, Kleihues., 2007). The time to progression is highly variable, ranging from less than 1 to more than 5 years before occurrence of GBM. Primary lesions typically affect older patients with a mean age of 62 years at diagnosis, whereas secondary GBM in contrast develop in younger patients with a mean age of 45. Phenotypically, primary and secondary GBM are indistinguishable. However, the two GBM subtypes display distinct genetic abnormalities, suggesting that their malignant transformation occurs through different genetic pathways. Primary GBM in adults is associated with epidermal growth factor receptor (EGFR) overexpression and mutation, loss of heterozygosity (LOH) of chromosome 10q, mutation of the phosphatase and tensin homology (PTEN) gene, and deletion of the p16 gene. Mutations in the p53 gene, LOH of chromosome 10q, and abnormalities in the pathway regulating the tumor suppressor Rb are frequently found in secondary GBM. Overall, these genetic alterations in both primary and secondary GBM result in overactivation of several mitogenic signaling pathways that ultimately leads to uncontrollable growth of the affected cells. (Ohgaki, Kleihues., 2007 and Stegh., et al., 2007)

The cellular origin of GBM is subject of intense investigation. Traditionally, it was believed that GBM arose from mature astrocytes, and that expression of progenitor cell markers was the result of de-differentiation during the process of malignant transformation. However, recent research suggests that the tumors may originate from malignant transformation of neural stem cells or related progenitor cells (Das, Srikanth, Kessler., 2008). In agreement with this theory, cancer cells with stem cell-like properties have been isolated from GBM tumors and cell lines. These so-called cancer stem cells (CSCs) only account for a small fraction of the tumor, but

exhibit classical stem cell properties such as an extensive proliferative potential, self-renewal, and multipotency. Furthermore, the isolated CSCs display pronounced tumorigenic behavior when implanted into immunocomprised mice, giving rise to tumors mimicking the phenotype and recapitulating all the different cell types of parent tumors. CSCs may therefore be the driving force of GBM growth through their unlimited growth potential. Accumulating evidence suggest that the CSCs may represent descendents of neural stem cells or related progenitor cells that suffered the initial carcinogenic insult, but still the possibility of de-differentiation of more mature astrocytes have not been disproved (Stiles, Rowitch., 2008). Thus, distinct proof of the cellular origin of GBM as well as their inherent CSCs still remains to be found.

Cancer stem cells

Normal adult stem cells have been described in small quantities in most of the body tissues, where they carry out functions of tissue maintenance and regeneration (Verstappen, J., et al., 2009). There are two properties that help to define a stem cell:

•self-renewal. Stem cells have unlimited replicative potential.
• multipotency. Stem cells have the ability to differentiate into the different cell types that compose the tissue of origin.

These properties are due to the ability of stem cells to perform both symmetrical and asymmetrical mitotic divisions. The former produces two identical daughter stem cells, while the latter give rise to a stem and to a more differentiated cell. This allows stem cells to provide cell replacement for the whole lifespan.
The idea that a subpopulation of stem cells may guide the development of the tumor dates back from the early twentieth century (Becker., Mc, and Till, 1963 and Furth, and Kahn 1937). This hypothesis arises from studies that assessed cancer cells heterogeneity in terms of both morphological and proliferative potential (Heppner., 1984.). Indeed, in cancer cell population only a small fraction is able to form colonies in semisolid culture. It is also known that xenotransplantation experiments (into immunocompromised mice) requires a large number of cells, indicating that only a small fraction of cells is equipped with tumorigenic capacity

(Hamburger and Salmon, 1977). Two models have been proposed to explain this heterogeneity (Figure2). The "stochastic" model proposes that all the cells within a tumor have tumorigenic capacity. The explanation why only a small part of them is able to regenerate the tumor *in vitro* and *in vivo* is therefore due to extrinsic factors such as experimental or microenvironmental conditions.

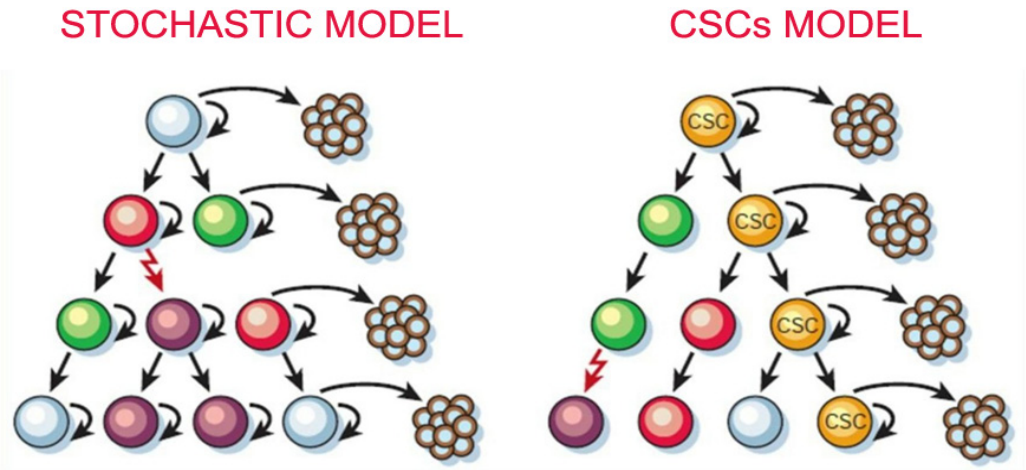

Figure 2. Two general models to explain cellular heterogeneity in solid tumors. According to the stochastic model there is a degree of heterogeneity among the tumor cells and most of them have the ability to form new tumors. According to the CSC model only a small population of cells (represented in yellow) can give rise to new tumors (Reya , et al.,2001).

According to "cancer stem cells" (CSC) model, instead, there is a specific subpopulation of cells capable of expressing tumorigenic properties. CSC in fact shares with normal tissue stem cells the ability to self-renew and generate differentiated progeny responsible for tumor formation and maintenance.

CSC existence was confirmed in 1997 by John Dick and colleagues who first isolated human leukemic CSC (Bonnet, and Dick,1997) . The experimental procedure adopted is analogous to that used for hematopoietic stem cells (HSC) isolation (Baum, et al., 1992 and Osawa, et al., 1996). $CD34^{+}/CD38^{-}$ cells were isolated by Fluorescence Activated Cell Sorting(FACS) from patients with acute myeloid leukemia and inoculated in immunodeficient mice (NOD/SCID) to test their tumorigenicity. The authors found that $CD34^{+}/CD38^{-}$ were able to regenerate the

leukemic compartment whereas, the $CD34^{+}/CD38^{+}$ more differentiated population, lack this ability. This study was followed by other leading to the possibility to identify CSC populations also in solid tumors including breast, central nervous system, prostate, lung, liver and colon cancer (Table1).

Cancer stem cells associated markers.

Tumor Type	Marker
Leukaemia	$CD34^{+}$, $CD38^{+}$
Breast	$CD44^{+}$, $CD24^{low}$, $ALDH^{+}$
Brain	$CD133^{+}$
Melanoma	$CD20^{+}$
Lung	$Sca1^{+}$, $CD45^{+}$ $Pecam^{+}$, $CD133^{+}$
Liver	$CD133^{+}$
Head and Neck	$CD44^{+}$
Colon	$CD133^{+}$
Stomach	$CD44^{+}$
Pancreas	$CD44^{+}$, $CD24^{+}$, ESA^{+}
Ovary	$CD44^{+}$

Table1. Cancer stem cells associated markers

Once having identified cancer cells with stem-like properties several assumptions about their possible role in cancer development have been made. One possibility is that mutations occur that alter self-renewing regulation in normal stem cells given the ability of stem cells to self-renew indefinitely while maintaining replicative potential. A second hypothesis is that these cells are more likely to accumulate mutations over time increasing chances of neoplastic transformation. However, CSC model identification has, led to new approaches in cancer experimental research. This is true especially in light of recent works that have been demonstrated CSC resistance to chemotherapy and radiotherapy. One of the most commonly

used methods for CSC enrichment from primary cultures of tumor cells, is the Hoechst 33342 dye exclusion (Goodell, et al.,1996 and Kondo, Setoguchi, and Taga, 2004) . Goodell and colleagues demonstrated that this phenomenon involves the multidrug resistance transporter (MDR1), a member of the ABC (ATP Binding Cassette) family transporters (Hirschmann-Jax, et al.,2004). Several studies (Nakai, et al.,2009 and Shervington, and. Lu, 2008) showed that the CSC associated chemoresistance is due to increased expression or activity of MDR1. Other gene expression studies have identified a correlation between CSC chemotherapy resistance and high expression levels of Breast Cancer Resistance Protein (BCRP1) multidrug resistance gene. Similarly, genes involved in DNA mismatch repair system as MGMT (methyl-guanine methyl transferase) and genes encoding antiapoptotic proteins such as Bcl-2, Bcl-XL and FLIP have been associated with chemoresistance (Liu, et al.,2006). As with chemotherapy, radiotherapy resistance has been linked to the CSC. In a recent paper has been shown that the stem cell subpopulation contributes to tumor radioresistance through more efficient checkpoint activation by DNA damage, compared to the remaining tumor population (Bao, et al., 2006). For the aforementioned reasons, CSC subpopulation can be considered responsible for tumor initiation, progression and spreading to other organs. Thus, CSC must be considered as a new target for therapy aimed at complete tumor healing (Figure 3).

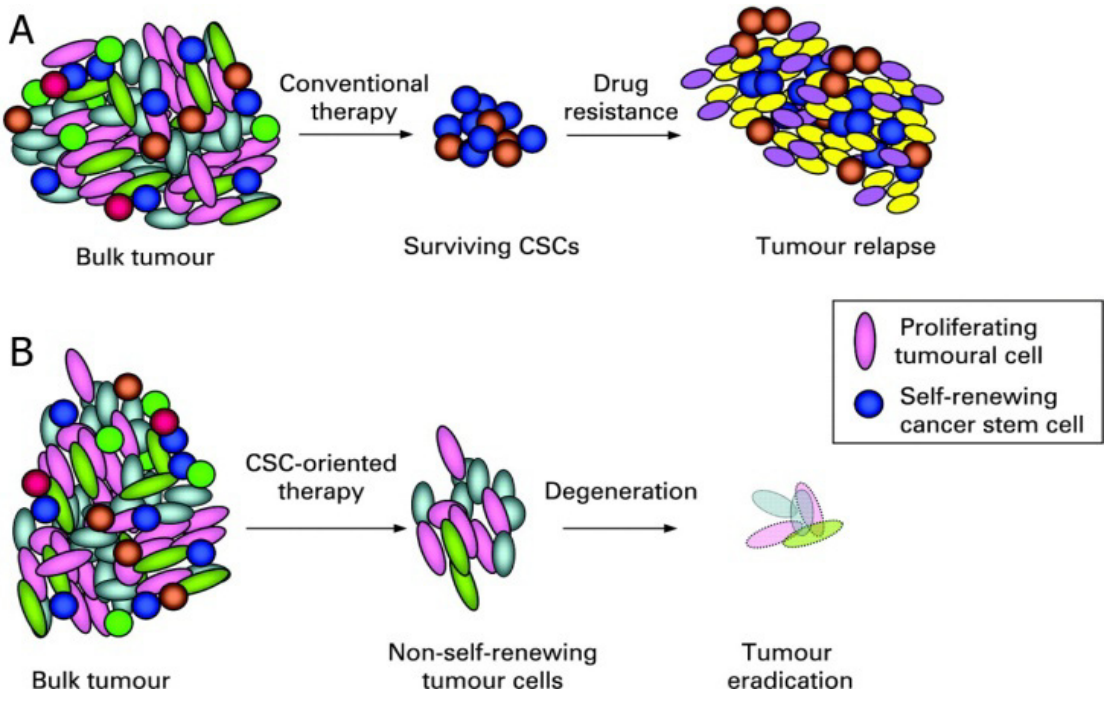

Figure 3. (A) Conventional therapy was mainly addressed towards the more mitotically active cells, thus resulting less effective on resting cells such as CSC. After an initial shrinkage the tumor tends to recur because of the small stem cell population remained alive. (B) A targeted therapy can selectively kill CSC thus eliminating tumor regenerative capacity (Ricci-Vitiani, L., et al.,2009) .

Isolation and characterization of Glioblastoma Stem Cells

In our laboratory, we have set up a procedure for the isolation of stem cells from glioblastoma specimens. We isolated undiffrentiated GBM-stem cells (GBM-SCs) from surgical specimens through mechanical dissociation of the tumor tissue and after several passages in a serum free medium supplemented with epidermal growth factor (EGF) and basic fibroblast growth factor (bFGF). Isolated GBM-SCs were expanded and characterized both *in vitro* and *in vivo*. We characterize the pool of GBM-SCs obtained, for the expression of stem cell markers, especially the transmembrane glycoprotein CD133/Prominin and for the presence of genetic alterations typical of GBM. Normal and malignant primitive neural cells express the transmembrane glycoprotein CD133, whose expression increases considerably in neural tumor tissues (Singh.,et al., 2003 and 2004). Previous reports suggested that tumorigenic cells in GBM are confined into the $CD133^+$ population (Singh.,et al., 2003 and 2004). These initial findings have been revisited in light of

recent studies showing that CD133 cells isolated from human and mouse gliomas are tumorigenic (Lochhead., et al 2008 and Wiesner., et al 2008). However, tumor xenografts generated in immunocompromised mice by $CD133^+$ cells showed higher resistance to radiation and chemotherapy, suggesting that $CD133^+$ cells could be a more aggressive tumorigenic population (Zeng., et al 2006 and McLendon., et al 2006). The complexity of the stem cell compartment in glial tumors is confirmed by the demonstration that $CD133^+$ cells isolated from human glioma coexpress the glial fibrillary acid protein (GFAP), a marker for differentiated glial cells (Phillips., et al 2008). Although the stem cell compartment of GBM may be not entirely defined by CD133 expression, Zeppernick et al. (2008) have shown that both the proportion of $CD133^+$ cells and their topological organization in clusters were significant prognostic factors for glioma patients, thus providing clinical support to the claim that these cells play an important role in tumor growth and resistance to therapy.

We also characterize the GBM-SCs for their specific multilineage differentiation capacity in a matrigel plus stem cells medium without growth factors or in serum medium: under these conditions they are able to generate a progeny of neural lineages.

The tumorigenic properties of GBM-SCs are confirmed *in vivo* by intracranical or subcutaneous cell injection in immunocompromised mice. GBM-SCs were able to generate a tumor identical to the human tumor in terms of antigen expression and histological tissue organization.

Altogether, these features of GBM-SCs indicate that they may provide a riliable *in vitro* and *in vivo* model for studying GBM response to treatments and for to identify specific transcripts enriched in GBM-SCs (Figure 4).

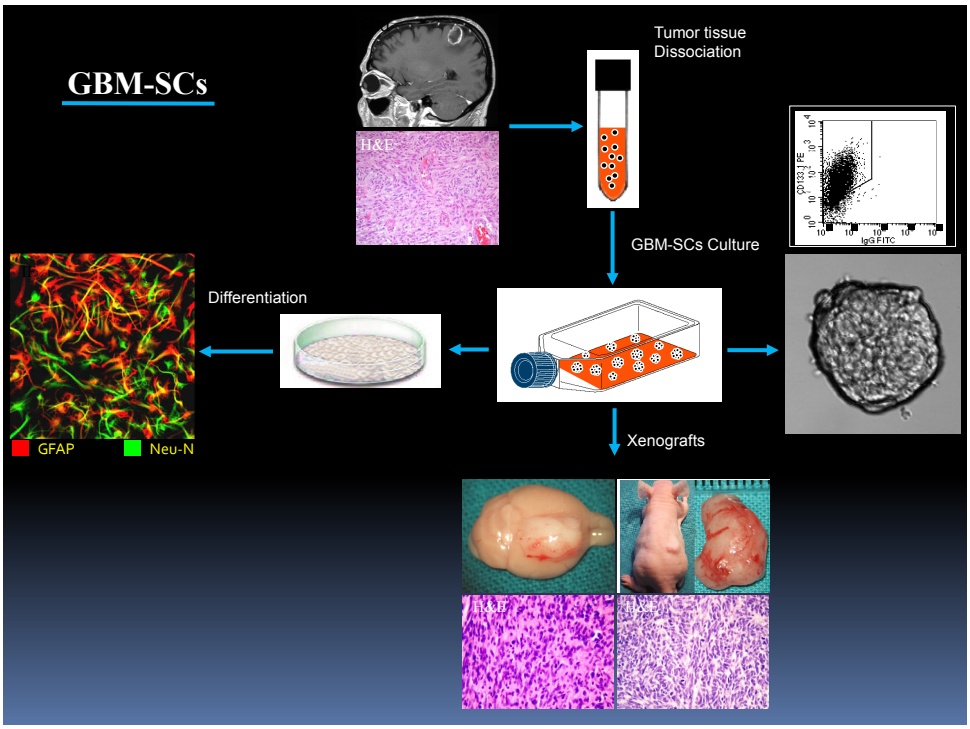

Figure 4. Schematic representation of isolation and characterization of GBM-SCs.

Expression profiling of microRNAs in GBM-SCs

We propose to identify therapeutic agents that efficiently kill GBM-SCs and we believe that this might lead to more effective treatments for the prevention of GBM relapse. For this purpose, we analyzed the expression profiling of microRNAs (miRNAs) in GBM samples in

order to identify those with potential importance in tumor biology. MiRNAs are small noncoding regulatory RNA molecules, with profound effects on a wide array of biological processes (Lee RC.;2004). After the discovery of the first miRNA in the roundworm Caenorhabditis elegans, these short regulatory RNAs have been found to be an abundant class of RNAs in plants, animals, and DNA viruses. MiRNAs are evolutionarily conserved, endogenous, small (19-25nt) non-coding single-stranded RNA molecules that negatively regulate gene expression in a sequence-specific manner. The human genome is predicted to encode as many as 1000 miRNAs, accounting for approximately 3% of the total number of human genes. The 5' portion of miRNA sequence containing bases two to eight, termed the "seed" region, is important in target messenger RNA (mRNA) recognition. MiRNAs negatively regulate target gene expression through complementarity between the miRNA seed sequence and the target mRNA 3' untraslated region (UTR). MiRNAs that bind with perfect complementarity to the protein encoding mRNA target the mRNA for destruction, whereas miRNAs with imperfect complementarity to the 3' UTR of the mRNA target, repress mRNA translation. Expression of approximately 30% of human proteins appears to be regulated by miRNAs. Through interactions with 3' UTR, miRNAs can modulate the expression of many genes simultaneously, often regulating individual signalling pathways at multiple levels.

MiRNAs are encoded by genes that are presumably transcribed into single or clustered miRNA precursors (pri-miRNAs) by RNA polymerase II or, in some cases, by RNA polymerase III and are converted in ~80 nucleotide pre-miRNA hairpin transcripts. The pre-miRNAs are processed to produce mature miRNAs that are incorpored in a ribonucleoprotein complex called the RNA-induced silencing complex (RISC). The core component of RISC is a member of Argonaute (Ago) subfamily proteins, of which there are four paralogs (Ago 1-4) in humans. RISC assembly follows a multi-step pathway. MiRNAs act by guiding the RISC complex to the target mRNA and direct RISC to down-regulate gene expression by mRNA cleavage or translational repression, depending on the specific RISC complex they assemble and the degree of complementary between the miRNAs and their mRNA targets. In humans, miRNAs mainly inhibit protein traslation of their target genes and only infrequently cause degradation or cleavage of the messenger RNA.

The biological role and *in vivo* functions of most mammalian miRNAs are still poorly understood.

In invertebrates, miRNAs regulate developmental timing, neuronal differentiation, cell proliferation, growth control, and programmed cell death (Johnston, Hobert., 2003 and Ambros et al., 1993). In mammals, miRNAs have been found to play a role in embryogensis and stem cell maintenance (Hannon et al., 2003), hematopoietic cell differentiation (Bartel et al 2004), and brain development (Miska et al .,2005 and Horvitz et al., 2004). MiRNA expression has been found to be deregulated in wide range of human diseases including cancer. However, it remains uncertain whether altered miRNA expression is a cause or consequence of pathological processes. The underlying mechanisms of why and how miRNAs become deregulated are largely unknown. Although bioinformatics approches can predict thousands of genes that are potentially targeted and regulated by miRNAs based on sequence complementary , only very few miRNA target genes have been functionally validated.

MicroRNAs and cancer

MicroRNAs have been recently demonstrated to play an important role in tumorigenesis.
Three important observations early in the history of miRNAs suggested a potential role in human cancer. Firstly, the earliest miRNAs discovered in the roundworm C. Elegans and the fruit fly Drosophila were hown to control cell proliferation and apoptosis. Their deregulation may therefore contribute to proliferative diseases such as cancer. Secondly, when human miRNAs were discovered, it was noticed that many miRNA genes were located at fragile sites in the genome or regions that are commonly amplified or deleted in human cancer. Thirdly, malignant tumors and tumor cell lines were found to have widespread deregulated miRNA expression compared to normal tissue (Lu, et al., 2005). The question remained whether the altered miRNA expression observed in cancer is a cause or consequence of malignant trasformation.
Several studies have shown that miRNAs could represent ideal therapeutic targets because of their involvement in biological processes such as development, cell differentiation, cell proliferation and cell death, all processes that are aberrant in cancer. The importance of miRNAs in cancer is highlighted by the observation that ~50% of miRNA genes are located in cancer associated genomic regions or fragile sites (Calin, 2004) which are frequently amplified or deleted in tumorigenesis. Moreover abnormal expression of miRNA has been linked with several cancers including glioma and its aggressive glioblastoma subtype (Ciafre et al., 2005).

During, the last decade, a unique set of cancer regulator miRNAs have emerged and these are divided into oncomiRs and anti-oncomiRs.

Up-regulated miRNAs may function as oncogenes by targeting and decreasing the expression of tumor-suppressor genes, while down-regulated miRNAs may function as tumor suppressors, impacting tumorigenesis by increasing the expression of oncogenes (Chen, 2005).

One example of miRNA with a tumorsuppressor function is miR-7. MiR-7 expression is frequently found decreased in GBM, while over-expression reduces cell proliferation, survival and invasiveness in cultured glioma cells (Kefas et al., 2008). The list of miR-7 confirmed targets include the epidermal growth factor receptor (EGFR) that play a major role in GBM tumorigenesis.

In contrast, miR-21 is almost invariably over-expressed in The list of miR-7 confirmed targetsinclude the epidermal growth factor receptor (EGFR) that play a major role in GBM tumorigenesis.

and a number of other tumor types (Calin and Croce, 2006), resulting in enhanced cell motility, migration and decreased apoptosis (Zhu et al., 2008; Gabriely et al., 2008). Growing evidences support the concept that miRNAs regulate oncogenes implicated in brain tumor formation. Godlewski and colleagues (2008) found that miR-128 levels were downregulated in glioma cells compared with normal brain tissue. They reported that increasing miR-128 expression leds to a decrease in the expression of the oncogene *Bmi-1*. Overexpression of miR-128 in glioma neurosphere cultures specifically blocks glioma self-renewal consistent with *Bmi-1* downregulation. Silber and colleagues (2008) were the first to discover that miR-124 and miR-137 are downregulated in high-grade gliomas compared with normal controls. These miRNAs are also upregulated during adult neural stem cell differentiation. The upregulation of miR-124 and miR-137 in tumor stem cell populations promotes neuronal differentiation of the tumor stem cells and inhibits their proliferation by inducing G0/G1 cell-cycle arrest. Gal and colleagues (2008) examined GBM stem (CD133-positive) and nonstem (CD133-negative) cells and found that miR-451, miR -486, and miR -425 were significantly upregulated in CD133-negative cells compared to CD133-positive cells. Transfection of GBM cells with these miRNAs inhibited neurosphere formation, and transfection with miR-451 resulted in neurosphere dispersion and inhibited GBM growth. MiRNAs have recently been shown to function as *bona fide* tumor suppressors. Shi et al.(2008) reported on downregulated miR-181a and miR-181b involved in glioma formation. Their study showed that these miRNAs

functioned as tumor suppressors. Transfection of these miRNAs into GBM cells inhibited proliferation in vitro, resulted in loss of anchorage-independent growth, induced apoptosis in glioma cell lines, and depressed the invasion of glioma cells *in vitro*. Although the investigation of miRNAs in brain tumors is still in its infancy, there is strong evidence mounting that miRNAs are integrally involved in brain tumor development and progression.

For these reasons , in the present project, we have planned to define the subset of miR genes that is aberrantly expressed in our GBM-SC lines when compared to normal neural stem cell lines. In a panel of hundreds of miR genes, we have identified miR-135b whose expression resulted downregulated in GBM-SCs when compared to neural stem cells. Functional evaluation of the dysregulated miR-135b has been performed by restoring its normal expression level in GBM-SCs using the inducible vector PTRIP-Zred. We studied the role of miR-135b in GBM-SCs and we found that miR-135b might exert a Tumor Suppressor function (TsmiR).

Cancer stem cells therapeutic implication

The most important therapeutic treatment for GBM is surgery. This procedure based on the premise that, although surgery is not a curative procedure, a major resection provides for a longer survival and better quality of life. Radiotherapy increases the duration of survival , but again is not a curative intervention. In the last 40 years, several clinical trials have examined the role of adjuvant chemoterapy in improving the survival of brain tumor patients. Chemotherapeutic agents have been administrated before (neo-adjuvant), during (concomitant) or after (adjuvant) radiotherapy. The additions of temozolomide to radiotherapy , resulting in a survival benefit with minimal additional toxicity., has became the standard treatment for newly diagnosed GBM.

CSC ability to maintain multipotency and tumorigenicity and their ability to faithfully reproduce the parental tumor in mice models of xenotransplantation, makes them an excellent model to study tumorigenesis and to evaluate the effectiveness of new cancer therapies. The development of new targeted therapy strategies will require a better CSC characterization in terms of their genomic and proteomic characteristics. Recent advances in cancer research have led to a better understanding of the molecular biology of cancer and the mechanisms that enable cancer cells to proliferate and survive. Target therapies for cancer refer to the use of drugs that preferentially target and inhibit specific molecular pathaways that allow cancer cells to continue to grow out of control and spread. Examples of targeted drug therapies for GBM

that are currently being evaluated in clinical trials include: tyrosine kinase inibitors, these drugs target a growth factor called EGFR that plays an important role in the growth and proliferation of GBM, angiogenesis inhibitors, these drug are designed to inhibit one or more of the growth factors that promote the formation of new blood vessels that provide essential nutrients for tumor cells and inhibitors of mTOR, the mammalian target of rapamycin that act as a central regulator of cell proliferation , angiogenesis and cell metabolism. There is accumulating evidence that the specific inhibition of molecules involved in proliferation and survival of cancer cells could lead to effective antitumour therapies. Phosphorylation, in particular, plays a major role in the regulation of signal transduction pathways that control proliferation, survival and cell death processes.

Reverse Phase Protein Array and drug screening

Post-translational modifications, such as phosphorylation, drive most of the cellular signal cascades and it has been shown that blockade of specific kinase activities is able to induce apoptosis in cancer cells. The analysis of the phosphorylation status of various proteins involved in survival/proliferation could eventually lead to the identification of new therapeutic targets. We have analyzed the activation of survival pathways associated to cancer and possibly contributing to GBM-SCs chemoresistance by the high throughput semi-quantitative technique, Reverse Phase Phosphoproteomic Array (RPPA) approach. RPPA represents a novel approach designed to conduct large-scale phosphoproteomic quantitative analysis. (Spurrier et al., 2008 and Ramalingam, and Nishizuka et al., 2008). This technology is a larger scale extension of western or dot blotting. Nano-amounts of protein lysates or laser capture microdissected biological sections are automatically spotted on nitrocellulose coated slides and then proteins of interest are detected by using specific antibodies. The high detection sensitivity permits to print on each spot less than one microgram of material, much less than that required in a Western blotting experiment. In addition this technology allows users to analyze hundreds of samples simultaneously on a single slide in a relatively short time. RPPA great potential lies in the possibility of molecularly characterize a large number of tumor samples, allowing the identification of prognostic/diagnostic factors as well as potential targets for novel therapies. RPPA has allowed us to obtain high content information about intracellular signaling networks and to define activated pathways in GBM samples from a large number of patients. We have

analyzed the expression and phosphorylation level of several proteins involved in signalling and cell physiology pathways that are abnormal in GBM and activate a cascade of intracellular events leading to cell proliferation, inhibition of apoptosis, angiogenesis, invasion and cytoskeletal rearrangement, such as EGFR-VEGFR, PI3K/Akt and Ras pathways.

We have treated GBM-SCs with 80 specific kinase inhibitors of those survival pathways in order to identify molecular mechanisms whose inhibition could overcome chemoresistance of these cells.

A synthetic derivative of staurosporine with antineoplastic activity, named UCN-01 or 7-hydroxystaurosporine, exerts a cytotoxic effect on the majority of our GBM-SC lines and it shows potent *in vivo* activity against a broad range of tumor types .

UCN-01

Seven-hydroxystaurosporine (UCN-01) is a derivative of the nonselective protein kinase inhibitor staurosporine that exhibits significant selectivity for protein kinase C (PKC) in comparison to a variety of other intracellular kinases and appears to be well tolerated *in vivo* at concentrations sufficient to achieve effective inhibition of PKC (Figg., et al 2005). UCN-01 was originally identified as a potent (<100 nmol/L) inhibitor of calcium-dependent protein kinase C (PKC)-α, -β, and -γ isoforms. It has also been described for, UCN-01 an antiproliferative activity in several human tumor cell lines (Akinaga et al., 1991; Seynaeve et al.,1993). Subsequent studies revealed that it also potently inhibits the DNA damage response regulatory kinases *chk*1(protein kinase that regulates the G2 checkpoint) (Ic50= 5-11nM) possibly *chk*2 (Ic50>1000nM) (Sarkaria., et al 2000.; Pommier Yet al 2002.; Schwarz., et al 2000) and phosphatidylinositide-dependent kinase 1 (PDK1) (Sato., Fujita ., Tsuruo ., 2002). Several studies suggest that UCN-01 is not only able to abrogate the G2 checkpoint induced by DNA-damaging agents but also, in same circumstances, UCN-01 is able to abrogate the DNA damage-induced S phase checkpoint (Bunch and Eastman,1997; Shao et al., 1997). Another interesting property of UCN-01 is its abitity to arrest cells in the G1 phase of the cell cycle. Several study in human epidermoid carcinoma or lung carcinoma have demonstrated that after incubation with UCN-01, these cells were arrested in G1 phase with Rb hypophosphosphorylation and p21/p27 accumulation (Akiyama et al., 1997). Chen et al (1999) suggest that Rb, but not p53, function is essential for UCN-01- mediated G1 arrest, but the exact role of Rb or p53 in the G1 arrest induced by UCN-01 is still unknown. In summary,

three different effects has been described for UCN-01 on tumor cells: (1) cell cycle arrest (This agent arrests tumor cells in the G1/S transition of the cell cycle and preventions of nucleotide excision repair by inhibition of chk1); (2) induction of apoptosis and (3) sensitization to DNA-damaging agents. Moreover, it has been demonstrated that UCN-01 is able to inhibit invasion and migration of human glioma cells (Fan., et al 2005) and to increase Temozolomide efficacy in both p53 wild-type and p53 mutant glioma cells (Pieper., et al 2001). UCN-01 inhibits cell growth in several *in vitro* and *in vivo* human tumor preclinical models. Several lines of evidence suggest that UCN-01 shows antitumor activity and might be a novel anticancer drug, which regulates the cell cycle of tumor cells. Therefore, phase I studies of UCN-01 as a single agent or as a modulator of several standard anticancer drugs have been conducted in the United States and Japan (Sausville et al, personal communication, 2002). UCN-01 showed unusual pharmacokinetic features in patients with cancer, which could be explained, at least in part, by the extremely high affinity with human alpha-1 acid glycoprotein (AAG). On the basis of these results, we propose the use of UCN-01 as a possible therapeutic strategy against GBM-SCs.

Methods

Glioblastoma stem cells isolation and culture.

Glioblastoma tissue specimens were obtained from adult patients undergoing craniotomy at the Institute of Neurosurgery, Catholic University School of Medicine in Rome. Glioblastoma stem cells were isolated through mechanical dissociation of the tumor tissue and grown as semiadherent neurospheres in a serum-free medium supplemented with epidermal growth factor (EGF) and basic fibroblast growth factor (bFGF) as previously described. Isolated cells were expanded and characterized both *in vitro* and *in vivo* for their stem-cell properties according to the following criteria: (1) ability to grow in clusters and maintain an undifferentiated state, as indicated by morphology and expression of stem-cell markers such as CD133, SOX2, musashi and nestin; (2) ability to differentiate under serum stimulation both into GFAP-positive astrocyte-like cells and into neurofilament expressing neuron-like cells; (4) generation of glial tumors upon orthotopic (intracerebral) transplantation in immunodeficient mice; (5) maintenance of chromosomal aberrations of the parental tumor.

Lentiviral Vectors

We used the pTRIPZ vector which has been engineered by Open Biosystems to be a Tet-On vector. The Tet-On® technology equips the pTRIPZ vector to provide for induced expression of a shRNAmir in the presence of doxycycline (www.clontech.com). For pTRIPZ-Red135b generation (TPZred), miR-135b precursor DNA was amplified from human genomic DNA. We subcloned the amplfied fragment spanning 650 bp into the lentiviral vector pTRIPZred under the control of the cytomegalovirus promoter (CMV). The primers used for amplification of pri-mir-135b are: CGGTCTAGACCATTGTGTGAGGCCTTT (Fw) and CCCGATATCACCCCCCAAATCT (Rv). PCR was performed under the following conditions: initial denaturation for 2 minutes at 94 ^{o}C, 35 cycles of denaturation for 15 second at 94 ^{o}C, annealing for 30 second at 56 ^{o}C, extension for 1minute and 30 second at 68 ^{o}C and 10 minutes at 68 ^{o}C for final extension. Then, the PCR products were determined by 1% agarose gel electrophoresis. For Tet-On inducible system pTRIPZ red vector act as responders to rtTA by inserting, in a lentiviral backbone, a tetracycline response element (TRE) upstream of a minimal promoter driving the transcription of Red Fluorescense Proteins RFP or RFP/mir-135b respectively. TRE consists of seven repeats of tet operator (tetO).

Glioblastoma stem cells lentiviral infection

Lentiviral particles were produced by calcium phosphate transfection protocol in 293T packaging cell line. The day before transfection 293T cells were plated at density of.. 1.2x10^{6} cells in a T75 cell culture flask. Cells were transfected with 20 µg of lentiviral vector, 13 µg of packaging vector (pPAX) and 7 µg of vescicular stomatitis virus protein G vector (pMD2G). $CaCl_2$ (125 mM) and HBS (2XHBS: NaCl 280 mM, KCl 10 mM, Na2HPO4 1.5 mM, D(+)glucosio 12 mM, HEPES 50 mM, pH 7.1) were included in transfection mix to promote calcium phosphate/DNA precipitates formation. 12 hours post-transfection culture medium, full of calcium phosphate precipitates, was replaced with fresh growth medium. 48 hours post-transfection, viral supernatant were filtered with 0.45 µm filter and used for the following GBM-SC samples infection.

For lentivirus infection GBM-SCs were plated as single cells in a 6-well culture plate at 80% of confluence. The day of infection the cells growth medium was replaced with 2 ml of filtered viral supernatant. Polybrene (4 µg/ml) was used to improve infection efficiency. Cell plates

were first centrifuged for 45 min at 1800 RPM at 37 ^{0}C and then were incubated over night at 37 ^{0}C. At the end of the infection, the cells were washed extensively and maintained in a serum-free medium supplemented with growth factors . The transduction efficiency was evaluated by cytofluorimetric analysis.

After lentiviral infection , GBM-SCs were selected by antibiotic resistance to puromycin. Successively infected cells were induced with the tetracycline analog doxycycline and, after two days, RFP-positive cells were flow-sorted and used for functional assay and target analysis. Cells were sorted by BD FACSAria cell sorter according to manufacturer's from facility instrument technicians. Several stable stem cell lines were developed from independent viral productions/infections and exhibited identical behaviors.

RNA isolation and Real-Time PCR

Total RNA was extracted with TriZol reagent at different time point (for a period of two weeks post-sorting). Fifty nanograms of RNA were reverse transcribed with M-MLV reverse transcriptase (Invitrogen) or TaqMan reverse transcriptase (Applied Biosystems) and cDNA was diluted 1:10 in the PCR reactions. Housekeeping gene and target gene reverse transcription was performed using oligo-dT primers (Invitrogen), while miRNA specific looped-primer was used for miR-135b reaction.

Relative quantitative Real-Time PCR was performed in a Real-Time Thermocycler (MX 3000, Stratagene) using the Brilliant SYBR Green QPCR Master Mix according to manufacturer's instructions. All PCR reactions were coupled to melting-curve analysis to confirm the amplification specificity. Non-template controls were included for each primer pair to check for any significant levels of contaminants. Each experiment was performed in duplicate for three times.

MicroRNA analysis for identification of newtarget of GBM-SCs

We used TargetScan (http://genes.mit.edu/targetscan), miRanda (http://www.microrna.org), and PicTar (http://pictar.bio.nyu.edu) for mir-135b target prediction. The targets were confirmed by BLAST alignment with the corresponding NCBI DNA data base for homologies between miRs and their target. Moreover, putative target were selected for their involvement in glioblastoma pathogenesis.

In *vitro* Growth Curve

Spheres were mechanically dissociated. Cells were then plated in 96-well plates in triplicate, and incubated at 37°C in a 5% CO_2 incubator. Cells proliferation was monitored by counting the cell and confirmed by using the CellTiter-Blue Viability Assay (Promega). Experiments were repeated three independent times.

Soft agar colony formation assay

Assays of colony formation in soft agar were done using standard protocols. Briefly, transduced GBM-SCs (500-1000 cells per well) were suspended in 0.35% Noble agar and were plated onto a layer of 0.7% Noble agar in 24-well tissue culture plates (Corning). The agar containing cells was allowed to solidify overnight at 37°C in 5% CO2 humidified atmosphere. Additional medium was overlaid on the agar and the cells allowed growing undisturbed for 2 weeks. Plates were stained with 0.5ml of 0.005% Crystal Violet for 1 hour. Visible colonies were counted with the aid of a microscope. Experiments were repeated three independent times.

***In vitro* cell migration assay**

The motility of transduced GBM-SCs was evaluated in 24-well transwell chambers (Costar), as directed by the manufacturer. Briefly, the lower chambers of the 24-well plate were filled with 500 µL of stem cell medium containing EGF and FGF2; 1×10^4 cells in 500 µL of the same medium was placed into the upper compartment of wells. The transwell chambers were incubated at 37°C in 5% CO2 humidified atmosphere for 24 h. The cells that had invaded to the lower surface of the polycarbonate membranes (8 µm pore size) were fixed, stained with Coomassie blue, and quantified by counting five microscopic fields (at ×100 magnification) per filter. Experiments were repeated three independent times.

Clonogenical assay

Glioblastoma spheres were dissociated by gently pipetting up and down to obtain a single cell suspension. In all, 3 and 10 cells were seeded in each well of 96-well plates in stem cell medium plus doxiciclina. After 3-4 weeks, each well was examined and the number of sphere/well was counted. Experiments were repeated three independent times.

Tube formation assay

The human umbilical vein endothelial cells (HUVECs) were seeded on MATRIGEL (BD Biosciences).
HUVECs were suspended in normal medium and in the conditioned medium derived from TPZred-135b infected cells with respect to the control cells. After several time, images of the cells were taken using an Electron microscope.

Tumor formation in vivo

The effects of miR-135b on in vivo tumor growth were tested in an intracranial glioma xenograft model. Infected GBM-SCs ($5x10^5$) were implanted intracranically into immunodeficent mice (n=6). The animals were sacrificed after 3 week of tumor implantation. The brains were removed,sectioned, and stained.

Phosphoproteomic analysis

A RPPA (Reverse Phase Protein Array) module consists of a solid support that can quantify proteins of interest previously immobilized onto nitrocellulose coated slides through the use of specific antibodies. Sample proteins immobilization was obtained through the use of an "Arrayer" tool that deposit (printing) microspot (about 30 nanoliters of sample) onto nitrocellulose slides. The immunostaining procedure, (staining) is automatically performed by an Autostainer. A portion of the printed slides are processed to detect the amount of total protein (used to normalize the antibody signal) by a fluorescence method. Once generated,

signal, is detected by a high resolution scanner. The images obtained are analyzed by a software that can automatically identify the spots and quantify their relative intensity.

Printing

This procedure is performed by an Aushon 2470 Arrayer that takes advantage from a 20 "pin" head (5x4) that permits samples spotting onto nitrocellulose coated slides. Samples are diluted 1:2 with print loading buffer (Tris-glycine 2x SDS, Invitrogen) containing 2.5% β-mercaptoethanol (Sigma-Aldrich). After being heated at 100°C for 5 minutes and loaded in four different dilutions (1:1, 1:2, 1:4 and 1:8) on a 384-well plate (Genetix), samples are then spotted on the appropriate slide (FAST slides, Whatman, Fisher) by the instrument. Protein concentration is one of the most important parameter, in fact, too small amounts of protein per-spot can give rise to false negative results, while to high amounts can cause signal saturation.

Protein quantification

All protein signals were normalized on the basis of total protein values. This parameter has been estimated by SYPRO Ruby Protein Blot Stain (Invitrogen). After slides printing some of them were selected for total protein determination as described below:

• Fixing solution incubation (7% acetic acid and 10%methanol).
• Washes (water) and SYPRO Ruby Blot Stain incubation for 30 minutes.
• One minute wash.

Slides are then dried at room temperature and then scanned with a fluorescence scanner (Vidar Systems Comporation, Revolution 4550).

Staining

Staining was performed using the TSA and DAB (Tyramide Signal Amplification, Diaminobenzidine, DAKO, Denmark) system of signal amplification. In this procedure, a primary antibody is detected with a biotinylated secondary antibody. This process allows a significant signal amplification useful for the detection of femtomolar antigen amount. Before the immunostaining, slides are incubated for 15 minutes with a stripping solution (Reblot mild antibody stripping solution, Chemicon) to promote antigenic sites exposure. After two PBS washes slides are treated for two hours with PBS containing powder I-block 0.2% (Applied

Biosystems/Tropix) and Tween-20 0.1%, in order to saturate nitrocellulose a specific binding sites. Before primary antibody staining, slides are subjected to a streptavidin pretreatment in order to saturate endogenous biotin eventually present in the sample. The entire staining procedure is automatically carried out using a DAKO Autostainer.

Data analysis

After staining, slides are scanned with a flatbed scanner (UMAX PowerLook, UMAX, Dallas, TX) at a 1800 dpi resolution and saved as *.TIFF image file using Photoshop 6.0 (Adobe , San Jose, CA). Images are then analyzed with the MicroVigene software 2.9.9.9 (Vigen Tech, North Bedford, MA).

Expression levels of each protein in the GBM-SC lines were "standardized" as follows: $(xn-\mu)/\sigma$, where xn represents the intensity of the single protein in the sample n, μ is the mean value and σ the standard deviation of the individual proteins intensity calculated for all samples analyzed**.** In this way data are represented as relative expression values between the several lines in a range between -1.5 and 1.5 standard deviations. Data hierarchical clustering was performed through the T-MEV (http://www.tm4.org) open-source program.

Anticorpi utilizzati nell'analisi fosfoproteomica

Nome	Ditta	Specie	Cat. #
Histone H3 (S10) Mitosis Marker	Upstate	Rabbit	06-570
ASK1 (S83)	CellSig	Rabbit	3761
Akt (S473)	CellSig	Rabbit	9271
Akt (T308)	CellSig	Rabbit	9275
Bad (S136)	CellSig	Rabbit	9295
c-Abl (T735)	CellSig	Rabbit	2864
Smad2 (S465/467)	CellSig	Rabbit	3101
FAK (Y397) (18)	BD	Mouse	611806
PAK1 (S199/204)/PAK2 (S192/197)	CellSig	Rabbit	2605
EGFR (Y1068)	CellSig	Rabbit	2234
c-Raf (S338) (56A6)	CellSig	RmAb	9427
EGFR (Y992)	CellSig	Rabbit	2235
ERK 1/2 (T202/Y204)	CellSig	Rabbit	9101
Met (Y1234/1235)	CellSig	Rabbit	3126
4E-BP1 (T70)	CellSig	Rabbit	9455
S6 Ribosomal Protein (S240/244)	CellSig	Rabbit	2215
PRAS40 (T246)	BioSource	Rabbit	44-1100
ErbB2/HER2 (Y1248)	CellSig	Rabbit	2247
Jak1 (Y1022/1023)	CellSig	Rabbit	3331
p70 S6 Kinase (T389)	CellSig	Rabbit	9205
PLCgamma1 (Y783)	CellSig	Rabbit	2821
4E-BP1 (S65)	CellSig	Rabbit	9451
EGFR (Y1045)	CellSig	Rabbit	2237
mTOR (S2481)	CellSig	Rabbit	2974
B-Raf (S445)	CellSig	Rabbit	2696
Adducin (S662)	Upstate	Rabbit	06-820
EGFR (Y1173)	BioSource	Rabbit	44-794
PKC alpha (S657)	Upstate	Rabbit	06-822
FAK (Y576/577)	CellSig	Rabbit	3281
Stat3 (Y705) (D3A7)	CellSig	RmAb	9145
PKA C (T197)	CellSig	Rabbit	4781
PKC zeta/lambda (T410/403)	CellSig	Rabbit	9378
GSK-3alpha (Y279)/beta (Y216)	BioSource	Rabbit	44-604
eIF4G (S1108)	CellSig	Rabbit	2441
PDK1 (S241)	CellSig	Rabbit	3061
Catenin (beta) (T41/S45)	CellSig	Rabbit	9565
NF-kappaB p65 (S536)	CellSig	Rabbit	3031
MARCKS (S152/156)	CellSig	Rabbit	2741
Ras-GRF1 (S916)	CellSig	Rabbit	3321
GSK-3beta (S9)	CellSig	Rabbit	9336
IkappaB-alpha (S32/36) (5A5)	CellSig	Mouse	9246
c-Kit (Y719)	CellSig	Rabbit	3391
IRS-1 (S612)	CellSig	Rabbit	2386
VEGFR 2 (Y996)	CellSig	Rabbit	2474
Stat1 (Y701)	CellSig	Rabbit	9171
CREB (S133)	CellSig	Rabbit	9191
Bad (S112)	CellSig	Rabbit	9291
Pyk2 (Y402)	CellSig	Rabbit	3291
Survivin (71G4)	CellSig	RmAb	2808
p27 (T187)	Zymed	Rabbit	71-7700
Stat5 (Y694)	CellSig	Rabbit	9351
p90RSK (S380)	CellSig	Rabbit	9341
Bcl-2 (S70) (5H2)	CellSig	RmAb	2827
MEK1/2 (S217/221)	CellSig	Rabbit	9121
SAPK/JNK (T183/Y185)	CellSig	Rabbit	9251
Estrogen Receptor alpha (S118)	CellSig	Rabbit	2515
PTEN	CellSig	Rabbit	9552
PTEN (S380)	CellSig	Rabbit	9551
p38 MAP Kinase (T180/Y182)	CellSig	Rabbit	9211
EGFR (Y1148)	CellSig	Rabbit	4404
Stat3 (S727)	CellSig	Rabbit	9134
Shc (Y317)	Upstate	Rabbit	07-206
FKHR (T24)/FKHRL1 (T32)	CellSig	Rabbit	9464
PDGF Receptor beta (Y716)	Upstate	Rabbit	07-021
VEGFR 2 (Y1175) (19A10)	CellSig	RmAb	2478
FKHR (S256)	CellSig	Rabbit	9461
c-Abl (Y245)	CellSig	Rabbit	2861
p70 S6 Kinase (S371)	CellSig	Rabbit	9208
MSK1 (S360)	CellSig	Rabbit	9594
PKC alpha/beta II (T638/641)	CellSig	Rabbit	9375
mTOR (S2448)	CellSig	Rabbit	2971

Kinase inhibitors library *in vitro* screening

For *in vitro* screening experiments GBM spheroids were subjected to mecchanicaly dissociation .After being counted with Trypan Blue dye in a Burker chamber to exclude death cells, 2000 cells per well were plated onto 96-well microplates in 80 µL of culture medium. Each different treatment were performed 24 hours after plating by adding 20 µL of culture medium.

Inhibitors included in the Biomol Library (Enzo Life Sciences/Biomol http://www.enzolifesciences.com/BmL -2832/kinase-inhibitor-library) were initially tested at a 5µM concentration. All inhibitors were resuspended in DMSO (dimethyl sulfoxide, Sigma-Aldrich Inc., Saint Louis, MO). Some samples were therefore treated with DMSO 0.1% as a vehicle control. Staurosporine was used as positive control.

Positive hits titration and combination with chemotherapeutics or commercially available inhibitors

Compounds that resulted effective in the first screening were then titrated using scalar concentrations (5µM , 2,5µM, 1,25 µM, 0,6µM, 0,3µM, 0,15 µM, 0,07 µM, 0,03 µM), in addition to the vehicle control (0.1% DMSO).

Again, selected compounds were tested *in vitro* in combination with conventional chemotherapeutic agent temozolomide (Sigma-Aldrich Inc.) at 500µM, 250µM and 125µM concentrations. In the same experiment, cells were treated individually and in combination with commercially available inhibitors. DMSO 0.1% was used as a vehicle control. UCN-01 (Sigma-Aldrich Inc.) dose-response treatment was conducted for the fourtheen lines of GBM-SCs at 10 µM, 5 µM , 1,25 µM, 0,6 µM, 0,3µM, 0,15 µM, 0,07µM and 0,03µM. DMSO 0.1% was used as a vehicle control.

Viability assay

In vitro viability was assayed measuring cellular ATP content by luminometry. To this end we used the chemiluminescence assay CellTiter-Glo™ (Promega Inc., Madison, WI) following

manufacturer instructions. This method takes advantage of cells ATP content to convert luciferin, the substrate of the enzyme luciferase, in an unstable compound. Before undergoing spontaneous oxidation the compound is able to emit photons in the 510-650 nm range of wavelength.

Viability was tested at different times of treatment. The intensity of the luminescence, proportional to cell viability, was measured by Victor 2™ (Wallac, Perkin Elmer Inc., Norwalk, CT) microplate reader. Vehicle control (DMSO 0.1%) luminescence values were averaged and arbitrarily set to 100%. The absolute values of luminescence for each treatment were then normalized with respect to vehicle control and then expressed as a percentage.

Tunel assay

Following procedure of a Roche protocol (Version 2, October 2001) for use with paraffin embedded sections, paraformaldehyde fixed material. Use at least two control and two test sections per slide (two groups – they should not be too close, that the reagents don't mix during the reaction). We examine sections under the microscope with dark field illumination before starting the experiment to choose sections you want to use for TUNEL staining (better looking sections) and for control sections. Tunel assay was performed on cells fixed in 4% paraformaldehyde-PBS at 20 min RT. Permeabilization of cells with 0,1% Triton-100 and incubate 5 minutes at room temperature. Washing cell in PBS and prepare the Tunel cocktail:

-40 µl of Labeling solution for one control

-180 µl of Labeling solution in a new eppendorf tube, plus 20 µl of Enzyme solution.

Mix thoroughly, but take care not to create many bubbles (vortex on medium, then spin down briefly). We added 50 µl of TUNEL cocktail on test sections, we put 40 µl of Labeling solution to control sections on one slide, we put PBS on the control sections on other slides.

Cover with parafilm pieces. Incubate in humidified chamber for 60 min. at 37ºC in dark (cover water bath with aluminum foil). Remove parafilm coverslips off the sections by pipeting PBS around the edge of parafilm until it floats, then lift it with tweezers. Wash 3 times in PBS for 3 minutes . Add DAPI staining as a final step for 60 min. at 37ºC in dark. Drain excess solution from the slide. Apply two separate drops of Gel Mount-DAPI on the sections, then carefully

lower the coverslip on sections. Let stand in dark for few minutes. We then observed DAPI stain with UV excitation, and observed TUNEL signal with Death Detection kit, Fluorescein, following the manufacture's instructions (Roche)

Western blotting

To determine, phospho-Akt (S473) (Cell Signaling), phospho-PKCα/βII (T638/641) (Cell Signaling), phospho-PDK1 (S241) (Cell Signaling) and phospho-cdc25 (Cell Signaling) expression levels, GBM spheroids were subjected to mechanical dissociation, after being counted $5x10^5$ cells were plated 6-well in 2 mL of culture medium. Samples were subsequently treated with 0.1% DMSO (Sigma-Aldrich), UCN-01 (Sigma-Aldrich) 1 μM.. Protein lysates were prepared by resuspending cells in a T-PER lysis buffer (Pierce) with 300 mM NaCl and Protease Inhibitor Cocktail and Phosphatase Inhibitor Cocktails I and II (Sigma-Aldrich) according to manufacturer instruction. After a 30 minutes of-ice incubation, cells were centrifuged for 10 minutes at 13000 RPM at +4°C. The recovered supernatant was then directly used for Western blotting experiments or stored at 80°C.
Protein concentration has been assessed using Bradford protein assay (Bio-Rad Laboratories, Richmond, CA), which is based on Coomassie Blue G-250 dye ability to change its maximum absorption wavelength from 465 nm to 595 nm in response to protein binding.
Proteins were subjected to electrophoresis on acrylamide gel containing SDS (Sodium Dodecyl Sulfate). NuPage Novex Bis-Tris gel 1.0 mm x 15 well 4-12% (Gibco Invitrogen Inc) were used. An equivalent of 20 μg of protein, supplemented with loading buffer NuPage LDS sample buffer (25mM Tris-HCl, pH 6.8, SDS 10%, 50% glycerol, 5% β-mercaptoethanol, 0.01% bromophenol blue, (Gibco Invitrogen Inc.) was incubated at 95°C for 3 minutes and loaded. SeeBlue Plus 2 (Gibco Invitrogen Inc.) was used as molecular weight marker. Electrophoresis were performed in MOPS (3-[N-morpholino]-propansulfonico) buffer at 120 V for about 2 hours.

Antibody	Manufacturer	Species/Isotype	CAT#	Dilution
Primary antibody				
Phospho-AKT	Cell Signaling	Rabbit Monoclonal IgG	4058	1:1000
Phospho-pkc α/βII	Cell Signaling	Rabbit Polyclonal IgG	9375	1:1000
Phospho-pdk1	Cell Signaling	Rabbit Monoclonal IgG	3061	1:1000
P-cdc25	Cell Signaling	Rabbit Monoclonal IgG	4901	1:1000
Secondary antibody				
Anti-Rabbit IgG HRP-Linked	Amersham	NA934		

Intracranial implantation of glioblastoma neurosphere cells (GBM-SCs).

Experiments involving animals were approved by the Ethical Committee of the Catholic University School of Medicine, Rome. NOD-SCID mice (4–6 weeks of age; CD1 NOD-SCID mice, Charles Rives, Italy) were implanted intracranially with 2 x 10^5 green fluorescence protein (GFP)-expressing GBM-SCs resuspended in 5 µl of serum-free medium containing 1 uM of UCN-01. Control mice were injected with equal number of GBM-SCs suspended in 5 µl of serum-free medium without adding UCN-01. For grafting, the mice were anesthetized with intraperitoneal injection of diazepam (2 mg/100 g) followed by intramuscular injection of ketamine (4 mg/100 g). The animal skulls were immobilized in a stereotactic head frame and a burr hole was made 2 mm right of the midline and 1 mm anterior to the coronal suture. The tip of a 10- µl Hamilton microsyringe was placed at a depth of 3.5 mm from the dura and the cells were slowly injected. After 8 weeks of survival, the mice were deeply anesthetized and transcardially perfused with 0.1 M PBS (pH 7.4), followed by 4% paraformaldehyde in 0.1 M PBS. The brain was removed, stored in 30% sucrose buffer overnight at 4°C, and serially cryotomed at 20 µm on the coronal plane. Sections were collected in distilled water, mounted on slides, and cover-slipped with Eukitt. Images were obtained with a Laser Scanning Confocal Microscope (IX81, Olympus Inc, Melville, NY).

Histological assessment of tumor xenografts.

The cranio-caudal extension of the brain area invaded by GFP-expressing GBM-SCs was assessed on serial coronal sections. Then, histological sections 120 mm apart were digitized; on each image, the brain region containing GFP+ cells was demarcated with the cursor and its area calculated by using commercially available software. To assess the tumor volume, each area of infiltrated brain was multiplied for the distance to the consecutive digitized section starting from the tumor epicentre to the cranial and caudal poles of the tumor, and partial volume values were added. The density of tumor cells was assessed by counting the number of GFP-positive GBM-SCs in 10 non-superimposing high power fields across the grafted striatum. Alternate sections were stained with hematoxylin and eosin (H&E) for morphological analysis.

Statistical analysis.

All statistical analyses were conducted using GraphPad Prism 4 program (GraphPad Software Inc., www.graphpad.com). *In vitro* experiments statistical significance was calculated by ANOVA test. *In vivo* experiments the differences in tumor volume and density of GBM-SCs between the UCN-01 treated group and control group were evaluated using the Student's *t*-test. Statistical significance was assigned to p values <0.05.

Results

Expression profiling of miRNAs in GBM-SCs revealed that miR-135b is significantly downregulated

We first studied the expression levels of miRNA in GBM-SC lines in comparison to two neural stem cell lines. Total RNA was extracted from 33 stem cell lines cultured in their standard (serum free) medium and biological replicates were analysed by microarray hybridization (Agilent microarray core facility-University of Ferrara, Italy) in duplicate experiments. MicroRNAs were ranked by relative dysregulation and a cutoff was set living approximately 10% of the total as "significantly dysregulated" miRNA genes for further analyses. More in

detail, we estimated the absolute level of our miRNAs in tumors and in normal samples based on the assumption that, as miNAs act by stoichometric pairing with target mRNAs, their absolute expression levels are a key factor for inferring their function in a given context. Approximately 10% of the miRNA genes analysed resulted dysregulated by a factor of two or more. Based on our microarray platform, we analysed 40-50 transcripts for absolute quantification. To identify those miRNAs involved in the tumorigenesis of GBM-SCs, we mesasured their expression by a quantitative Real-Time PCR approch. We found that several miRNAs are consistently down-regulated in GBM-SC lines.

Among these, miR-135b resulted one of the most significantly down-regulated miRNA with the most homogeneous profile (Figure 1A).

Sample ()*	T1	T28	T62	T30pt	T30p	T23p	T23C	T148	T83.2	T83	T70	T87	T151	T147	T74	T68	T76	T61	NS5p16	NS5p17
hsa-miR-888		0.01	0.01	0.01	0.01	0.06	0.04	0.01	0.01	0.01	0.01	0.01	0.01	0.01	0.02	0.01	0.01	0.01	1.106	1.031
hsa-miR-891a	0.01	0.01	0.01	0.01	0.01	0.1	0.1	0.01	0.02	0.01	0.01	0.01	0.01	0.01	0.01	0.01	0.01	0.01	1.074	1.036
hsa-miR-891b	0.01	0.01	0.01	0.1	0.01	0.1	0.05	0.01	0.04	0.08	0.01	0.01	0.01	0.01	0.01	0.03	0.01	0.01	1.017	0.939
hsa-miR-363	0.07	0.01	0.03	0.03	0.01	0.4	0.18	2.04	79.4	0.01	0.89	0.07	1.25	0.62	8.62	11.1	1.31	0.02	142.9	123.8
hsa-miR-592	0.01	0.01	0.01	0.03	0.01	0.88	0.08	0.07	0.02	0.02	0.01	0.38	0.01	0.28	0.01	0.1	0.29	0.04	1.484	1.203
hsa-miR-18b	0.27	1.31	0.86	1.49	1.07	1.7	1.02	6.55	4.03	0.15	1.37	0.6	0.49	0.92	1.5	1.34	0.52	1.08	12.71	11.54
hsa-miR-135b	204	22.8	16.2	1.18	2.81	70.8	5.26	78.8	27.5	0.21	6.16	24.7	2.01	108	1.54	9.48	0.53	0.13	256.4	225.2
hsa-miR-20b	10.9	25.1	9.17	13.8	10.3	25.6	9.77	42.5	50.9	2.66	20.2	6.8	6.41	11.1	24.1	15.1	2.42	10.5	127	109.2
hsa-miR-219-5p	32.6	9	4.01	1.32	0.76	15.7	2.84	0.48	0.56	0.39	8.42	4.47	0.68	0.33	0.78	2.98	1.5	1.41	31.66	29.05
hsa-miR-455-3p	24.4	46.1	12.5	18.3	18.3	0.01	18.4	3.42	8.77	22.3	59.2	9.75	15.2	20.5	20.4	12	3.69	8.06	54.18	58.77
hsa-miR-17	22.4	59.8	21.2	26.9	24.2	60.4	22.6	114	39.5	5.45	40.9	17.2	12.4	26.9	42.4	22.1	10.9	24.3	109.9	92.33
hsa-miR-199b-5p	5.13	12.8	6.89	1.67	47.9	0.01	0.64	0.18	0.17	2.89	0.04	0.49	80.2	0.01	1.85	0.07	0.06	0.09	0.01	0.01
hsa-miR-199b-3p	14.7	7.96	5.04	16.1	141	0.14	0.47	0.57	0.34	38	0.05	0.43	179	0.45	1.5	0.04	0.01	0.08	0.184	0.136
hsa-miR-31	2.77	0.01	1.55	67.1	14.8	0.01	0.01	0.01	0.17	59.1	0.01	0.01	0.01	19.3	2.38	0.01	2.13	5.23	0.01	0.01
hsa-miR-183	4.69	0.18	2.45	7.61	10.9	0.01	0.01	3.1	3.79	3.11	51.9	2.16	0.01	0.8	0.16	0.01	0.07	20.8	0.01	0.01
hsa-miR-96	21.5	0.78	7.9	41.5	34	0.08	0.01	6.48	11.3	9.31	106	5.09	0.07	2.47	0.56	0.01	0.25	86.5	0.01	0.01
hsa-miR-196b	0.23	0.02	0.12	4.91	6.85	7.15	11.3	21.3	0.32	0.65	0.31	0.2	0.49	0.18	1.73	4.45	0.17	7.88	0.01	0.036
hsa-miR-148a	66.2	1	5.02	0.25	3.52	13.2	6.22	13.7	3.48	12.4	1.18	1.02	36.8	4.41	21.3	40.2	12.5	7.6	0.01	0.01
hsa-miR-29b	141	24	45.5	585	231	139	80.3	19.5	35.4	138	41.8	30.2	47.3	98.5	273	114	54.8	500	12.72	16.92
hsa-miR-21	788	932	458	3337	3167	311	592	54.4	310	956	1112	339	600	1329	5921	1324	509	2188	240.1	290.8
hsa-miR-193a-3p	6.41	6.83	0.47	55	20.4	9.77	3.57	9.59	3.46	18.3	11.5	7.44	23.3	4.61	65.1	19	5.27	33.3	0.194	0.1
hsa-miR-365	9.92	14.1	6.74	36.5	19.1	24.9	11.7	11.9	2.41	12.8	9.46	10.2	30	3.27	78.5	28.2	8.87	68.4	6.591	5.526
hsa-miR-29a	319	60.7	126	1084	406	219	168	42.8	92.3	227	118	126	171	204	532	181	156	775	84.68	66.55
hsa-miR-100	170	38.2	25.1	374	176	115	47.4	31.3	31	184	117	39.5	143	124	470	75.9	48.9	71.8	35.4	31.81
hsa-miR-27a	56.4	92.1	54.9	200	447	119	55.6	8.93	98.7	207	75.6	46.4	254	198	596	166	35.4	145	20.66	21.1
hsa-miR-10b	18.7	0.1	7.75	8.53	6.09	3.14	3.44	21.4	9.75	13.7	6.33	5.2	29	0.98	21.4	8.63	0.01	0.19	0.01	0.01
hsa-miR-23a	69.8	104	82.3	208	491	162	71.9	9.11	140	300	120	89.8	298	239	753	225	96.8	231	27.62	26.62
hsa-miR-550*	4.68	3.35	3.27	1.05	1.3	10.1	3.11	2	1.04	0.66	2.58	2.74	1.27	0.67	1.64	2.95	7.35	4.56	1.732	1.298
hsa-miR-22	72.7	31.8	23.6	171	130	51.5	8.84	12.9	15.3	62.4	56.8	33	84.5	165	174	136	101	237	30.77	34.27
hsa-miR-193b	9.58	15.5	7.13	18.7	11.5	21.9	8.8	8.08	1.93	18	8.33	17	14.5	2.02	39	33	30	52.3	7.668	6.721
hsa-miR-29c	60.7	16.2	12.1	77.3	32.8	73	26.8	10.1	8.52	29.7	28.5	30.2	19.7	37.1	68.9	69.9	20.5	119	15.98	15.45

Figure 1. A) Expression profiling of miRNAs in GBM-SC lines compared to NSC lines. In green, miRNAs down-regulated, in red miRNAs upregulated. MiR-135b resulted the most down- regulated with the most homogeneous profile.

Relative quantification by Real time PCR confirmed the downregulation of miR-135b in GBM-SCs (Figure 1B).

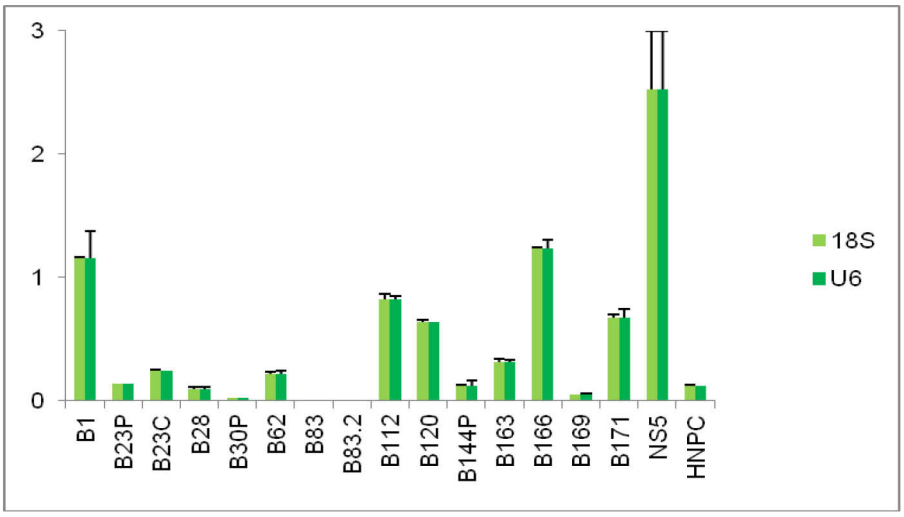

Figure 1. B) Relative miR-135b expression levels in GBM-SCs. Histogram shows down-regulated levels of miR-135b mRNA .

At this point we decided to investigate miR-135b function in the biology of GBM.
Functional evaluation of the dysregulated miR-135b was performed with a strategy aimed at restoring its normal expression levels in GBM-SCs.
For this purpose, we used a lentiviral inducible system in order to observe the effects of miR-135b soon after its enforced expression, avoiding possible counter selection phenomena.
We used the pTRIPZ vector (Figure 2A) which has been engineered by Open Biosystems to be a Tet-On vector. The Tet-On® technology equips the pTRIPZ vector for induced expression of a shRNAmir in the presence of doxycycline (www.clontech.com). There are two main components on the pTRIPZ vector enabling induction: the tetracycline response element (TRE) and the transactivator. The TRE, modified from its natural state to consist of a string of operators fused to the CMV minimal promoter, exhibits reduced basal expression and tighter binding to the second component, the transactivator. The pTRIPZ transactivator, known as the reverse tetracycline transactivator 3 (rtTA3), binds to and activates expression from the TRE promoter in the presence of doxycycline.

The rtTA3 transactivator is a modified version of the wildtype in two ways. First, unlike the original tetracycline transactivator, the rtTA3 is modified to bind to thr TRE in the presence of doxycycline rather than in its absence. Secondly, there are three mutations within the transactivator that increase its sensitivity to doxycycline by 25-fold over the initial rtTA, without increasing background activity (Das, *et al.* 2004).

GBM-SCs were infected either with the pTRIPZred and with its derivative pTRIPZred-135b vector, where the pri-mir-135b was cloned in the 3'untranslated region of the Red Fluorescent Protein (RFP). After infection, cells were selected with puromycin and then, induced with the tetracycline analog doxycycline and, after four days in culture, RFP-positive cells were flow-sorted and used for functional assays (Figure 2B). Overexpression of miR-135b (>500-fold) was confirmed on doxycycline induced GBM-SCs by real-time-PCR one day post-sorting and monitored over 3 weeks (Figure 2C).

A)

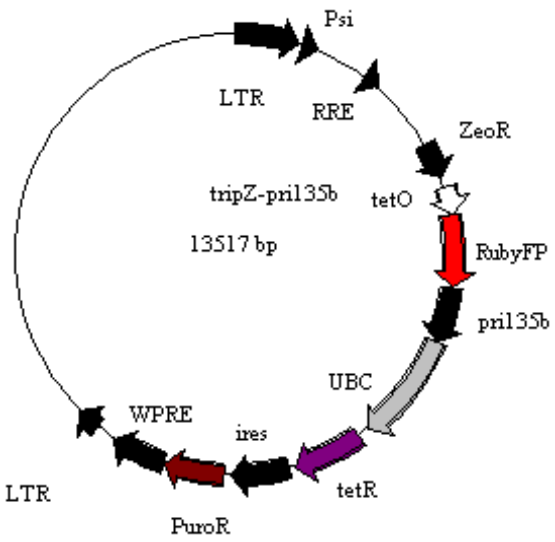

B)

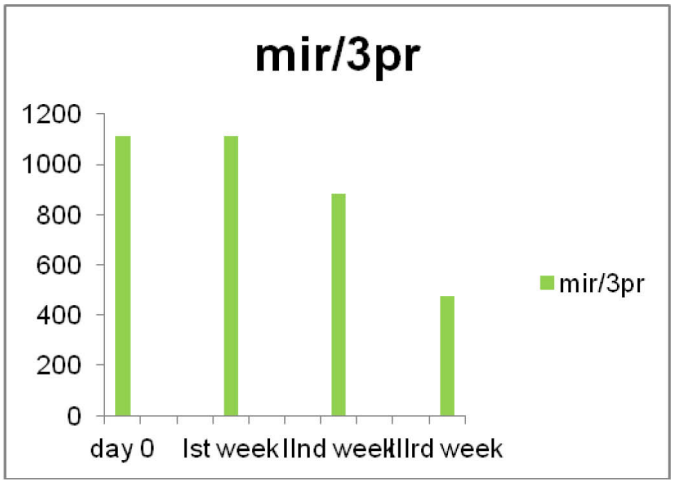

C)

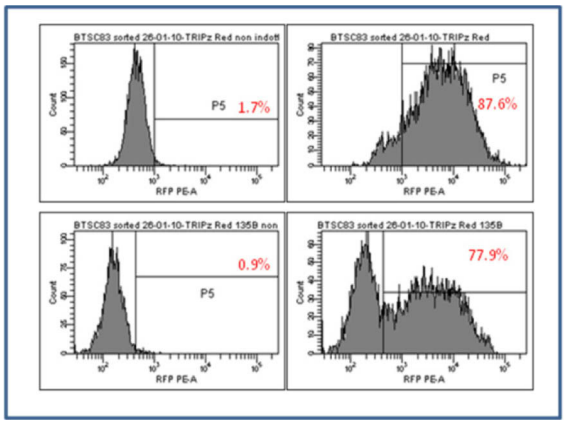

Figure 2. A) Schematic description of the pTRIPZ vector which has been engineered by Open Biosystems B) Facs analysis of flow-sorted GBM-SCs infected with pTRIPZred and pTRIPZred135b vectors 4 days after doxycycline induction C) Relative quantification of miR-135b on infected GBM-SCs.

MiR-135b overexpression inhibits GBM-SCs malignancy

We assessed the effects of miR-135b ovrexpression on GBM-SCs proliferation, migration and colony-forming ability. We performed functional assays on flow-cytometry sorted RFP-positive cells. The proliferation assay showed that pTRIPZred-135b-transduced (pTRIPZred-135b) cells have a significantly reduced growth compared to TRIPZred-transduced cells (pTRIPZred).

MiR-135b overexpression inhibits cell proliferation in GBM-SC lines # 30pt, # 83, and # 1 (Figure 3).

GBM-SC line # 30 pt

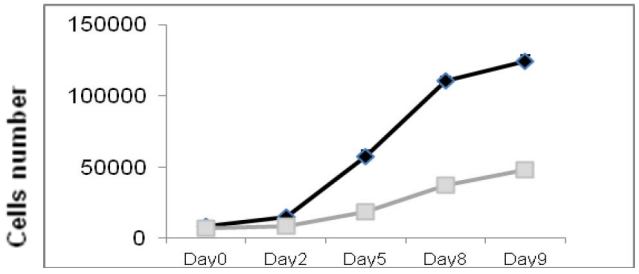

GBM-SCs line # 83

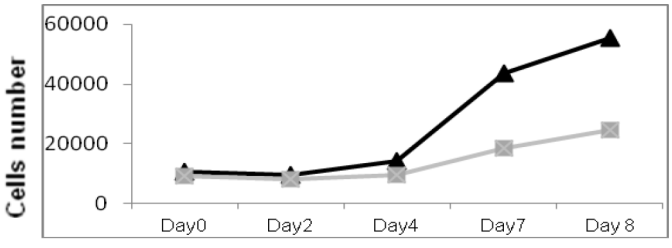

GBM-SC line # 1

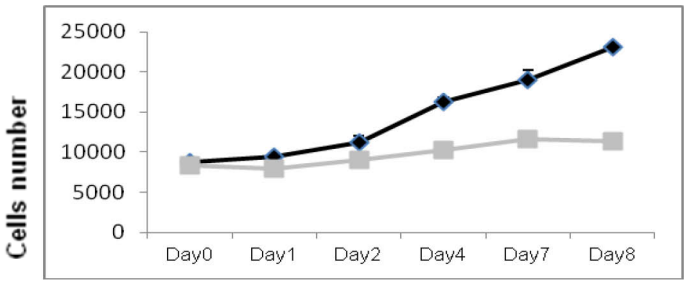

Figure 3. Overexpression of miR-135b significantly reduced the *in vitro* proliferation of GBM-SCs. Growth curves of GBM-SCs infected with pTRIPZred (black) and pTRIPZred-135b (grey) vectors.

High-grade gliomas exhibit aggressive behavior, which is manifested by rapid cellular migration under specific *in vitro* culture conditions (Chuang., et al .2004.; Manning and Sontheimer et al ., 1999). Using a standard "transwell chamber" assay where it is possible to count migrating cells through Comassie Blue staining, we found that enhanced expression of miR-135b significantly reduced the migration rate of pTRIPZred-135b cells compared to control pTRIPZred cells (Figure 4).

A)

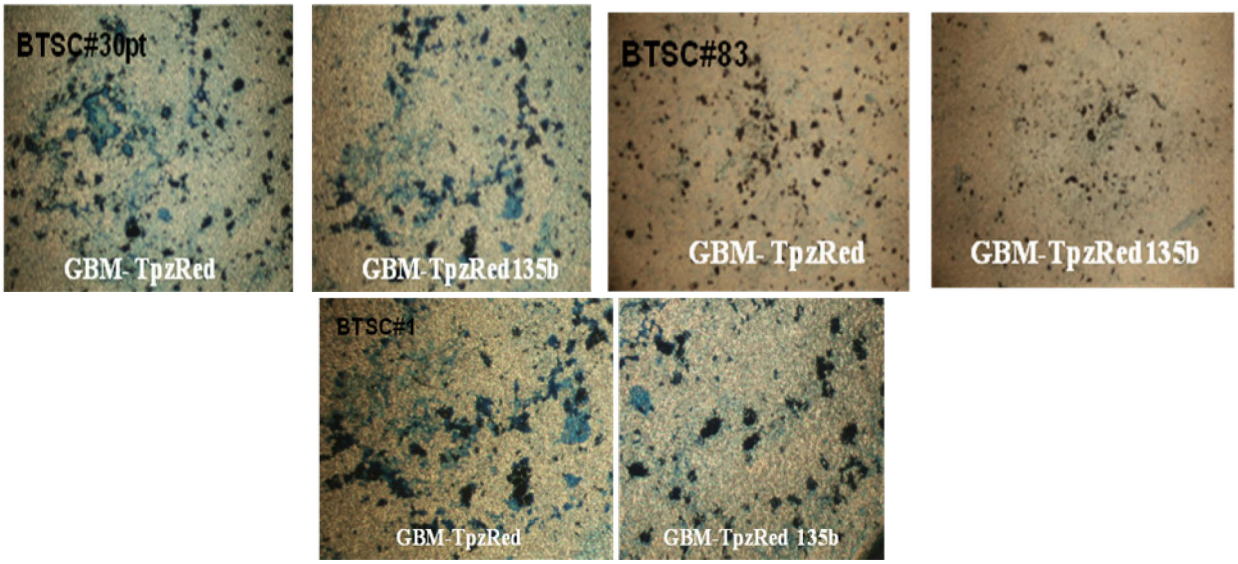

B)

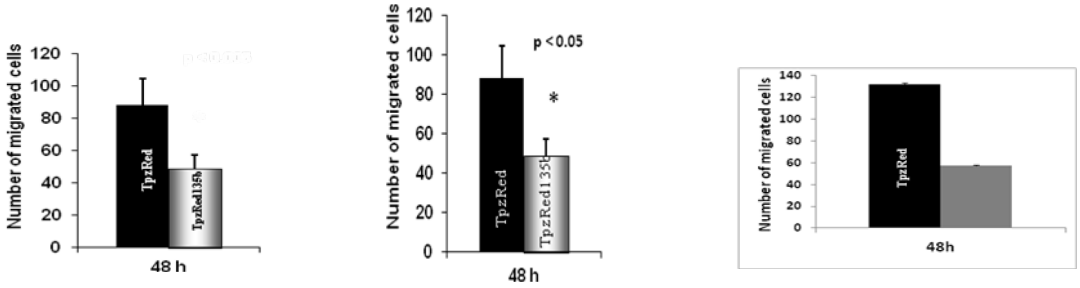

Figure 4. Overexpression of miR-135b attenuates the *in vitro* migration of GBM-SCs. A) Rapresentative contrast images showing migrating GBM-SCs. B) Number of migrating cells 48 hours after plating(GBM-SC lines # 30pt, # 83, and # 1).

.

The same cells used for the migration assay were used to assess whether reinforced expression of miR-135b does influence the ability of GBM-SCs to grow in an anchorage-independent manner. To this aim we plated doxycyclin induced infected cells in soft agar and, after 14 days, plates were stained and colonies were counted. We found that pTRIPZred-135b cells are able to form significantly less colonies than control cells (Figure 5).

GBM-SCs # 30 pt

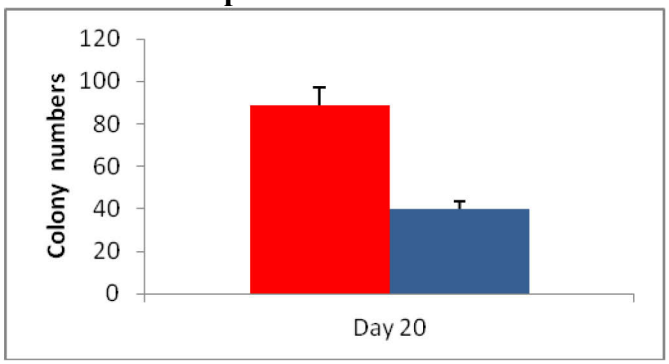

GBM-SCs # 83

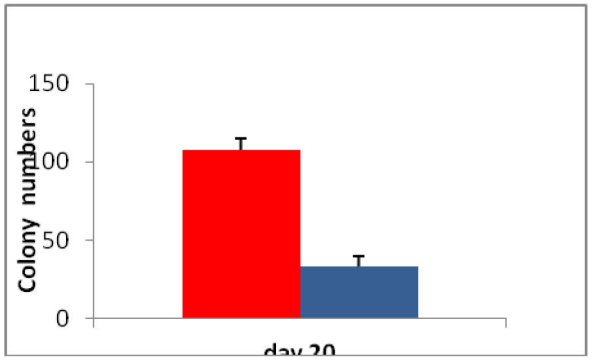

GBM-SC # 1

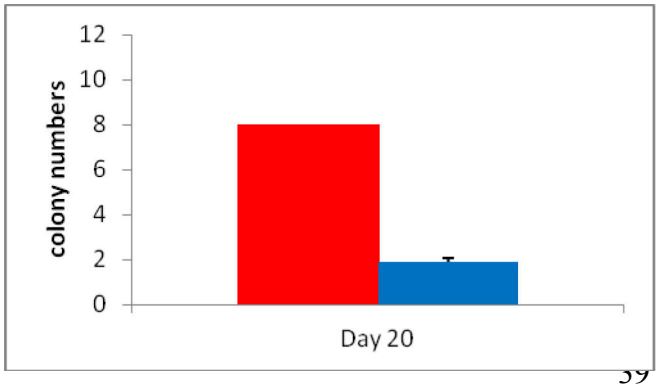

Figure 5. Overexpression of miR-135b attenuates the *in vitro* anchorage-independent growth of GBM-SCs. Graphs show the number of colonies formed in semisolid medium by GBM-SCs transduced with the indicated constructs and treated with doxycyclin to induce the transgene.

Moreover, we demonstrated that overexpression of miR-135b significantly reduced the number of clones in a clonogenesis assay, which is an in vitro model for cell trasformation (data not shown). These results identify a critical role of miR-135b in the regulation of GBM progression, suggesting that it might act as a tumor-suppressor factor. To understand more deeply the mechanisms by which this miRNA can behave as a tumor-suppressor, we tried to establish whether any of its putative targets play a crucial function in GBMa pathogenesis. We identified, among the target genes predicted by TargetScan software (Tan, 2009), some transcripts with specific roles in GBM progression. First, we investigated angiopoietin-2 (Ang-2) as putative miR-135b target, as it results, by TargetScan predictions, the most probable one and also because of the crucial role played by angiopoietin molecules in the growth and vascularization of GBM.

Although immunoblotting analysis of angiopoietin-2 on infected cells did not give significant resuls, tube formation assay showed that human umbelical vein endothelial cells (HUVECs) are able to significantly form less vessel-like stuctures in the conditioned medium of pTRIPZred-135b cells than in that of control cells (Figure 6). As Ang-2 mediates the formation of tube-like structures in capillary endothelial cells (an event which leads to angiogenesis), we can suppose that miR-135b, directly or indirectly targeting Ang-2, inhibits angiogenesis in GBM-SCs. We investigated others genes predicted by TargetScan and experimentally validated results by Immunoblotting (data not shown). Since we have not confirmed any miR-135b target yet, we will perform a microarray analysis to identify miR-135b targets in our GBM-SCs.

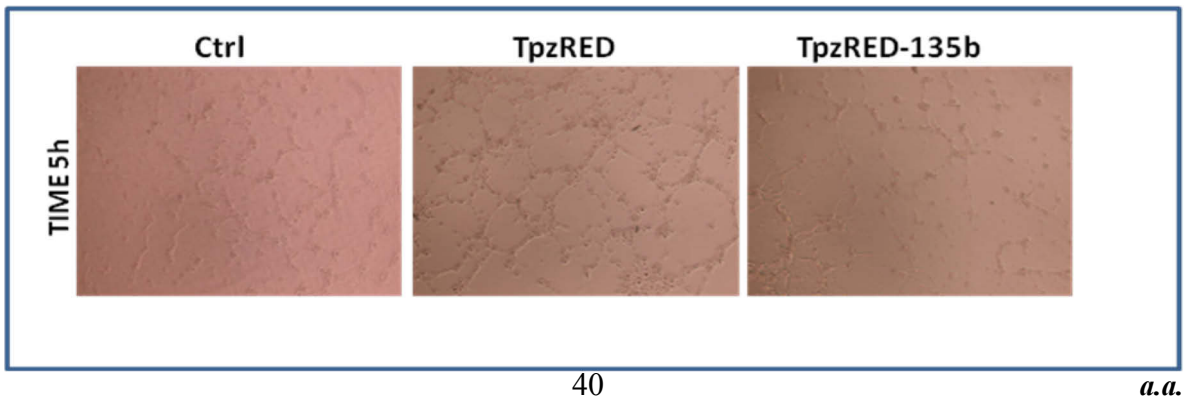

Figure 6. Electron microscope images of tube formation assay with HUVEC cells cultured on pTRIPZred and pTRIPZred-135b medium. After 5 hours of culture, HUVECs form significantly less vessel-like structures in the presence of pTRIPZred-135b conditioned medium than in control cells medium.

MiR-135b overxpression significantly decreses *in vivo* tumor growth

Having confirmed that the overexpression of miR-135b provokes a decrease in the tumorigenic properties of GBM-SCs, we endeavored to translate our findings in an *in vivo* GBM model. For this purpose, we grafted an equal number of pTRIPZred and pTRIPZred-135-b GBM-SCs into the brain of NOD/SCID mice. Mice were euthanized 3 weeks later, the tumors were dissected and analyzed. We observed that the degree of brain invasion was significantly reduced in mice grafted with TRIPZred-135b GBM-SCs compared to control mice (Figure 7). Altogether, these data confirm that miR-135b acts as a tumor suppressor in GBM development.

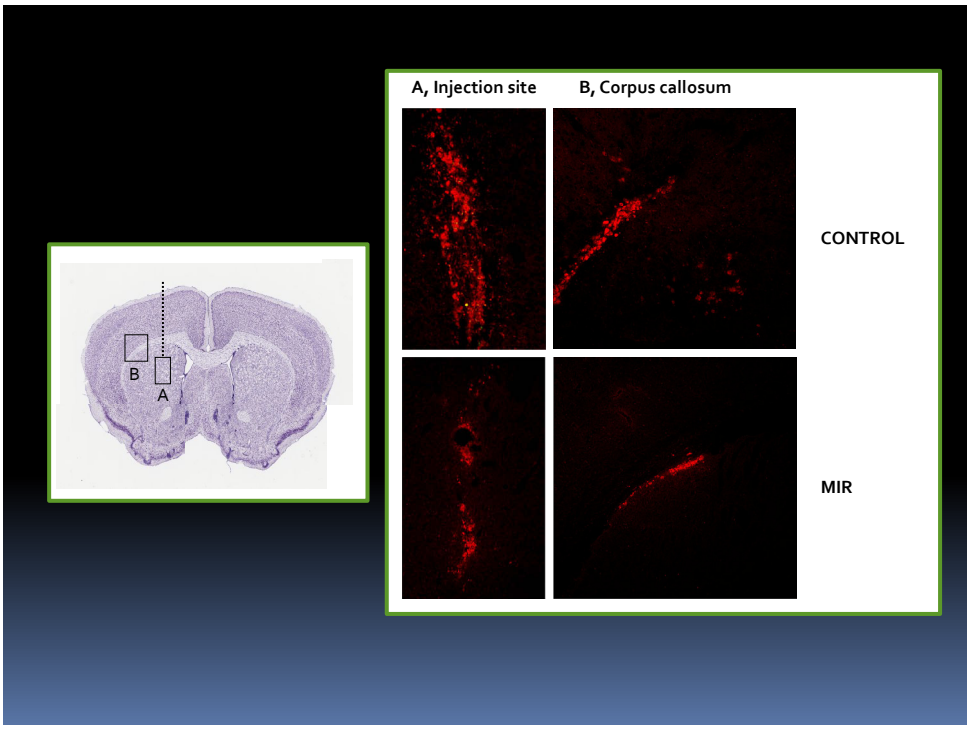

Figure 7. Effects the overexpression of miR-135b on the growth of tumors.

By 3 weeks after grafting, control mice showed more tumor cells invasion in the corpus callosum in comparison to pTRIPZ-red135b

Phospoproteomic analysis of GBM-SCs

We analyzed the activation of survival pathways associated to cancer and possibly contributing to GBM-SCs chemoresistance by the high throughput semi-quantitative technique, Reverse Phase Phosphoproteomic Array (RPPA). By RPPA, it is easily possible to create an activation map of different signal transduction pathways, testing GBM-SC samples with a panel of antibodies directed against phosphorylated epitopes of various kinases and their substrates. This analysis revealed a complex panel of kinase activities (figure 8) and was not possible to identify a single target protein common to all GBM-SC lines. These data reflect problems in identifying molecular targets for multifactorial diseases such as cancer, in which various individuals with different genetic abnormalities share similar histology and clinical course.

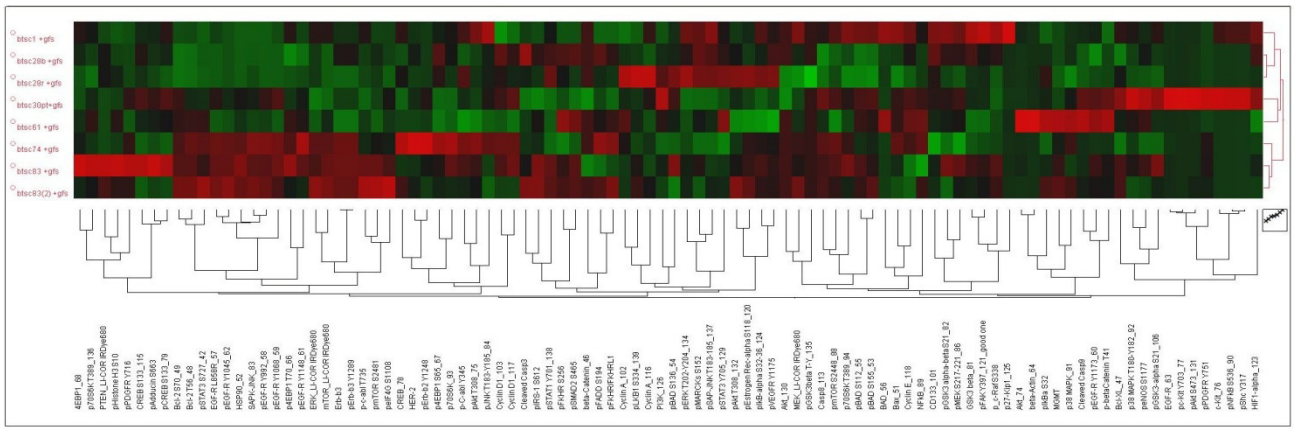

Figure 8. Representative RPPA analysis performed on GBM-SC samples.

Our results show high phosphorylation level of some proteins related to EGFR, VEGFR and their downstream pathways PI3K/AKT (AKT, GSK3, mTOR, Bad, p70S6K, PKC) and Ras (MEK, p38MAPK, p70S6K). Although with this analysis we could not find clear correlations between specific activated pathways and GBM subtype, in line with the extreme heterogeneity

of this tumor, we evaluated the possibility to overcome chemoresistance of GBM-SCs by treatment with specific inhibitors of those survival pathways.

To better understand the different characteristics of each of our GBM-SC line in terms of kinase activation and phosphorylation state we decided to directly test their *in-vitro* sensitivity to a panel of kinase inhibitors, to functionally test the importance of various molecular targets belonging to different signal transduction pathways for GBM-SC.

Screening of a kinase inhibitors library revealed 4 compounds that negatively affect the viability of GBM-SCs

Libraries of synthetic compounds with known specificity have been screened *invitro* with the aim to study the sensitivity of tumor cells to the inhibition of a specific signal transduction pathway and the consequent development of targeted drug therapies. The ability to test *in vitro* such a particular cell model, as the GBM-SC model, with a library of kinase inhibitors, provides additional benefits to the study of aberrations in signal transduction pathways. This experimental approach allowed to assess and discover the importance of pathways directly involved in tumor progression and maintenance, in a cellular system that is the ideal target for cancer therapy.

We tested the effect of a series of 80 kinase inhibitors that belong to a commercial chemical library (Enzo Life Sciences/Biomol http://www.enzolifesciences.com/BML-2832/kinase-inhibitor-library) on a panel of 7 GBM-SC lines previously isolated in our laboratory. The human GBM cell line T98G was used as control. The Biomol library specifically contains inhibitors of tumor cell proliferation, metabolism and/or survival, such as BTK, CaM Kinase, CDK, CKI/II, EGFR, GSK, IKK, Insulin Receptor, JAK, JNK, MAPK, MEK, MLCK, Pi3-Kinase, PDGFR, PKA, PKC, RAF, SAPK, Src-family and VEGFR.

Table 1 shows the library compounds and their corresponding molecular targets.

INHIBITORS	MOLECULAR TARGETS
PD-98059	MEK
U-0126	MEK
SB-203580	p38 MAPK
H-7	PKA, PKG, MLCK, and PKC.
H-9	PKA, PKG, MLCK, and PKC.
Staurosporine	Pan-specific

AG-494	EGFRK, PDGFRK
AG-825	HER1-2
Lavendustin A	EGFRK
RG-14620	EGFRK
Tyrphostin 23	EGFRK
Tyrphostin 25	EGFRK
Tyrphostin 46	EGFRK, PDGFRK
Tyrphostin 47	EGFRK
Tyrphostin 51	EGFRK
Tyrphostin 1	Negative control for tyrosine kinase inhibitors.
Tyrphostin AG 1288	Tyrosine kinases
Tyrphostin AG 1478	EGFRK
Tyrphostin AG 1295	Tyrosine kinases
Tyrphostin 9	PDGFRK
HNMPA (Hydroxy-2-naphthalenylmethylphosphonic acid)	IRK
Damnacanthal	p56 lck
Piceatannol	Syk
PP1	Src family
AG-490	JAK-2
AG-126	IRAK
AG-370	PDGFRK
AG-879	NGFRK
LY 294002	PI 3-K
Wortmannin	PI 3-K
GF 109203X	PKC
Hypericin	PKC
Ro 31-8220	PKC
Sphingosine	PKC
H-89	PKA
H-8	PKA, PKG
HA-1004	PKA, PKG
HA-1077	PKA, PKG
HDBA (2-Hydroxy-5-(2,5-dihydroxybenzylamino)benzoic acid)	EGFRK, CaMK II
KN-62	CaMK II
KN-93	CaMK II
ML-7	MLCK
ML-9	MLCK
2-Aminopurine	p58 PITSLRE beta1
N9-Isopropyl-olomoucine	CDK
Olomoucine	CDK
iso-Olomoucine	Negative control for olomoucine.
Roscovitine	CDK
5-Iodotubercidin	ERK2, adenosine kinase, CK1, CK2,
LFM-A13	BTK

SB-202190	p38 MAPK
PP2	Src family
ZM 336372	cRAF
SU 4312	Flk1
AG-1296	PDGFRK
GW 5074	cRAF
Palmitoyl-DL-carnitine Cl	PKC
Rottlerin	PKC delta
Genistein	Tyrosine Kinases
Daidzein	Negative control for Genistein.
Erbstatin analog	EGFRK
Quercetin dihydrate	PI 3-K
SU1498	Flk1
ZM 449829	JAK-3
BAY 11-7082	IKK pathway
DRB (5,6-Dichloro-1-b-D-ribofuranosylbenzimidazole)	CK II
HBDDE (2,2',3,3',4,4'-Hexahydroxy-1,1'-biphenyl-6,6'-dimethanol dimethyl ether)	PKC alpha, PKC gamma
SP 600125	JNK
Indirubin	GSK-3beta, CDK5
Indirubin-3'-monoxime	GSK-3beta
Y-27632	ROCK
Kenpaullone	GSK-3beta
Terreic acid	BTK
Triciribine	Akt signaling pathway
BML-257	Akt
SC-514	IKK2
BML-259	Cdk5/p25
Apigenin	CK-II
BML-265 (Erlotinib analog)	EGFRK
Rapamycin	mTOR

Table 1. The list of inhibitors included in the Biomol library and their relative molecular targets

GBM spheroids were subjected to mechanical dissociation in order to obtain a single-cell suspension ensuring reproducibility in the number of cells plated in each well (coefficients of variation < 10%). Cells were plated in triplicate for each treatment and after 24 hours they were treated with the 80 Biomol inhibitors at 5 μM concentration. We examined the assay plates using the CellTiter-Glo® Luminescent Cell Viability Assay after 72 and 96 hours of treatment. This method is based on cellular adenosine triphosphate (ATP) content.

Following a supervised analysis, we found that the majority of compounds tested were not toxic for our GBM-SCs, while only 4 inibitors reduced GBM-SCs viability by 50% or more, both at 72 and 96 hours of treatment, as compared to DMSO treated control wells (figure 9).

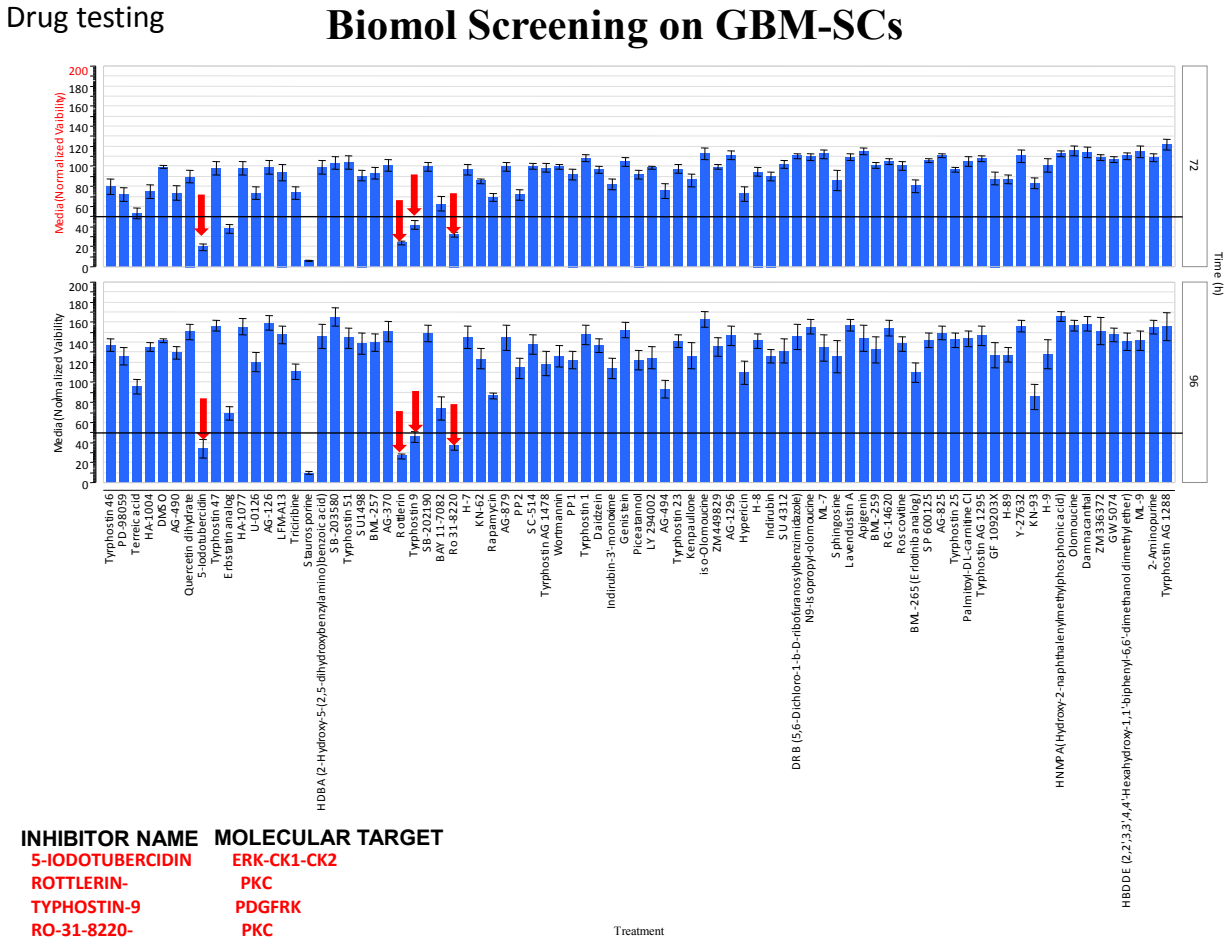

Figure 9. Cell death induction by kinase Biomol inhibitors on GBM-SCs after 72 and 96 hours of treatment

Inhibitors that showed an effect on GBM-SCs are : tyrphostin-9 and 5-iodotubercidin, whose targets are, respectively, the plated-derived growth factor receptor tyrosine kinase (PDGFR) and the extracellular signal-regulated kinase (ERK); RO 31-8220 and Rottlerin, whose target is the protein kinase C (PKC). The specificity of kinase inhibitors is not only due to their tridimensional structure, but also to the concentration at which they are used. The vast majority of synthetic inhibitors directly interacts with the kinase ATP-binding pocket (ATP-competitive), or avoids the conversion from the inactive to the active state. The ATP-binding

pocket is an enzymatic site that possess highly conserved amino acid molecules among the hundreds of kinases expressed by eukaryotic cells. Therefore, the concentration used in each treatment may be crucial in influencing the spectrum of specificity of each inhibitor.

Since our aim was to identify selective inhibitors of kinases responsible for GBM-SCs survival and proliferation, we wanted to check whether the Biomol compounds could negatively affect cell viability even at lower doses than the starting 5 μM concentration.

To this aim, we generated concentration-effect curves and calculated the IC_{50} values for the 4 compounds which resulted to reduce GBM-SCs viability.

Even with different degrees of sensitivity, GBM-SC lines similarly responded to the lower doses of inhibitors with IC_{50} values ranging between 1.5 and 2.5 μM concentration. The concentration decrease led to the disappearance of growth inhibition or death induction on GBM-SCs, probably indicating that effects observed at higher concentrations are not specific or toxic.

Table 2 shows the IC_{50} values of tyrphostin-9, 5-iodotubercidin, RO 31-8220 and Rottlerin on GBM-SC lines.

GBM	IC_{50}uM tyrphostin-9	IC_{50}uM iodotubercidin	IC_{50}uM RO 31-8220	IC_{50}uM Rottlerin
1	1.25	2.5	2.5	2.5
28	2.5	1	1.25	5
30pt	1.25	2.5	2.5	2.5
61	2.5	5	5	5
74	2.5	2.5	2.5	2.5
76	5	5	2.5	5
83	2.5	1.25	2.5	2.5

Table 2. Calculated IC_{50} values of tyrphostin-9, 5-iodotubercidin, RO 31-8220 and Rottlerin on GBM-SCs.

Only the RO 31-8220 analog UCN-01 significantly inhibits GBM-SCs proliferation/survival

Since the potential of new compounds in the treatment of gliomas is likely the association with established chemotherapeutic regimens, we tested the *in vitro* ability of the 4 Biomol compounds to potentiate chemotherapy on GBM-SCs. The rationale behind these regimens implicates that it is possible to achieve better effects while maintaining doses which are tolerated by patients. To this aim, we evaluated whether low concentrations of our kinase inhibitors, although not effective alone, could enhance the cytostatic or cytotoxic effects of temozolomide, the most commonly used chemotherapeutic agent against GBM.

Unfortunately, after combination treatments, we did not obtain a significant impairment in cell viability as compared to single agents administration (data not shown). In order to define signal transduction pathways involved in GBM-SCs survival and proliferation, we decided to test analogs of the 4 inhibitors acting at different levels of the same pathway.

Our attention was focused on molecules already used in clinical trials, as we were particularly interested in approaches with a relatively straight possibility of translation to clinical settings.

For PDGFR, some inhibitors were already approved by the FDA (Food and Drug Administration) such as Imatinib and Sunitinib. Even if these inhibitors are used in phase I/II studies for the treatment of GBM, they did not affect the viability of GBM-SCs; moreover, they do not specifically inhibit the tyrosine kinase activity of the receptor, having in fact at least another important target (c-kit for Imatinib and VEGFR for Sunitinib).

Even if the pharmacological inhibition of ERK is possible through the use of MEK inhibitors, its upstream kinase which mediates its activation, we excluded the importance of this target in GBM-SCs since two major inhibitors of MEK (PD98059 and U-126) already used in vitro resulted not effective in our study. The low relevance of the ERK pathway in GBM-SCs was confirmed by using a specific ERK inhibitor peptide *in vitro* (data not shown).

Inhibitors of one or more isoforms of PKC have been successfully tested in GBM cell lines and in pre-clinical studies. We treated our cells with ten of these inhibitors, including Calphostin C, an inhibitor of the regulatory site for diacylglycerol (DAG) binding and phorbol esters;

GO6983, a fast acting and lipid soluble inhibitor and tamoxifen, a selective modulator of the estrogen receptor.

They resulted effective in all the GBM-SCs lines tested but at doses between 5 and 10 μM concentration (data not shown).

Finally, only the RO318220 analog UCN-01 resulted to significantly impair GBM-SCs viability. This molecule is a staurosporine derivative with a 100 times higher *in vitro* IC_{50} and is well tolerated *in vivo*. Its known molecular targets are: the serine-threonine kinase Chk1, the protein kinase C (PKC) and the 3'-phosphoinositide-dependent kinase-1 (PDK-1). UCN-01 *in vitro* treatment of GBM-SCs was effective albeit with a wide range of sensitivity (IC_{50} values between 0,01 and 0,6 μM concentration). Table 3 shows the calculated IC_{50} for each line.

Our results demonstrate that it is probably necessary to hit more targets to affect tumor growth.

GBM line #	**UCN-01 IC_{50} (uM)**
1	**0.6**
28	**0.6**
166	**0.6**
188	**0.6**
61	**0.3**
62	**0.3**
68	**0.3**
76	**0.3**
74	**0.1**

83.2	**0.1**
148	**0.1**
151	**0.1**
30	**0.07**
83	**0.07**

Table 3. Calculated UCN-01 IC_{50} for several GBM-SCs after 96 hours of treatment.

In order to confirm the signaling pathways inhibited by UCN-01 in our tumor stem cell system, we first divided GBM-SCs lines analyzed in 4 groups corresponding to different degrees of sensitivity to the compound: low, medium-low, medium-high, high. We chose one representative GBM-SC line for each group and perform Immunoblotting to evaluate the signaling pathway/s inhibited by UCN-01 .

Figure 10 shows the 4 representative GBM-SC lines chosen: UCN-01 titration curves and UCN-01 IC_{50} values of for each line.

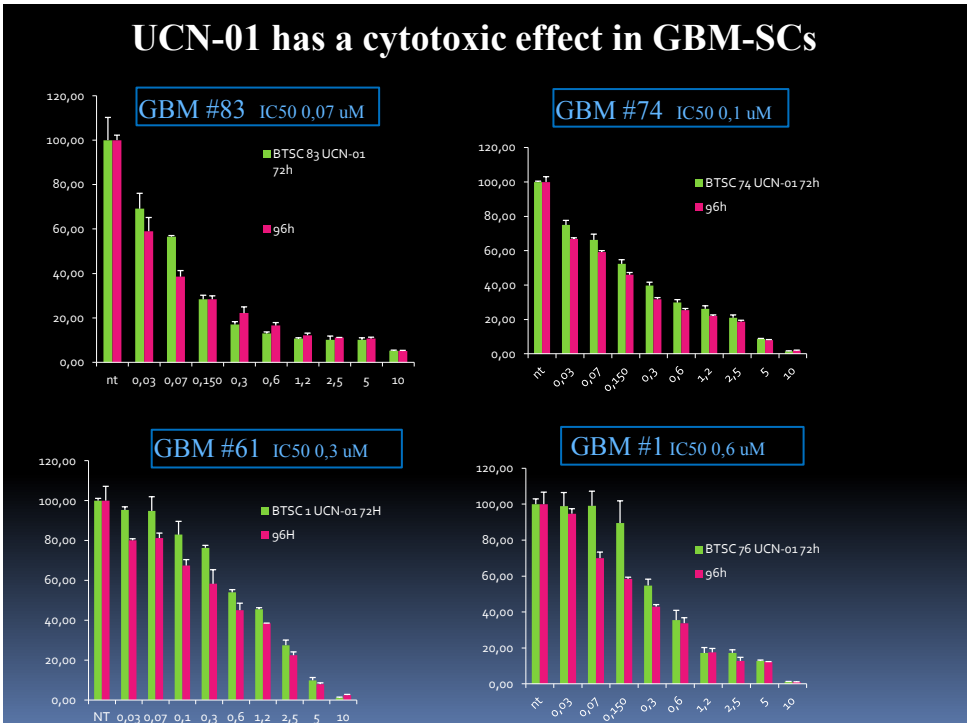

GBM#	Ic50-µM UCN-01
1	0.6
61	0.3
74	0.1
83	0.07

Figure 10. Top: titration curves of UCN-01. Bottom: UCN-01 IC_{50} values of the four representative GBM-SC lines chosen

Immunoblotting analysis revealed that, in all the representative lines, UCN-01 mostly inhibits Chk1, as its target molecule, the cyclin-dependent kinase Cdc25, resulted phosphorylated in non-treated compared to treated cells. Other UCN-01 targets in our GBM-SCs are: PKC and also AKT which is the substrate of PDK1 (Figure 11). These results confirm that UCN-01 affects GBM-SC proliferation/survival through the simultaneous inhibition of Chk1, PKC and PDK1.

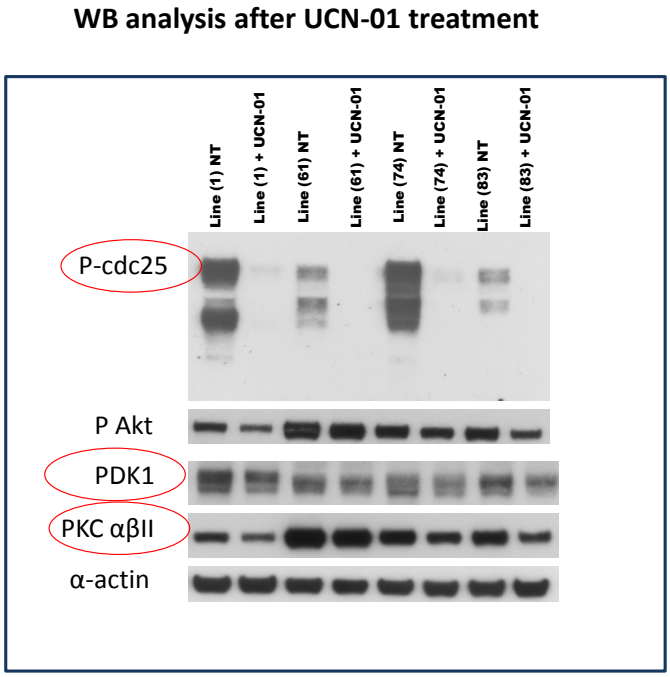

Figure 11. Immunoblotting analysis of the 4 representative GBM-SC lines non-treated and treated with 1 μM concentration of UCN-01 for 24 hours. Actin was used as loading control.

UCN-01 induces apoptosis in GBM-SCs

A number of tumor cells have been reported to undergo apoptotic cell death when treated with chemotherapeutic agents as etoposide, camptothecin or cisplatin. This finding indicates that apoptosis plays a critical role in chemotherapy- induced tumor cell killing and also suggests that blockade of the apoptosis-inducing pathways could be another mechanism for multidrug resistance (MDR). Based on the drug- and apoptosis- resistance mechanisms, we evaluated by Tunel Assay (Roche) whether UCN-01 effect on GBM-SCs proliferation/survival correlates with apoptosis induction. GBM-SCs of the 4 representative lines were treated with 1 μM concentration of UCN-01 for 24-48-72 and 96 hours. Immunofluorescence analysis on Tunel assayed cells revealed that UCN-01 induced apoptosis in all the lines. Percentages of apoptotic

cells were dependent on the different degree of sensitivity of each line to the compound. Figure 12 shows an example of UCN-01-induced apoptosis on one GBM-SC line.

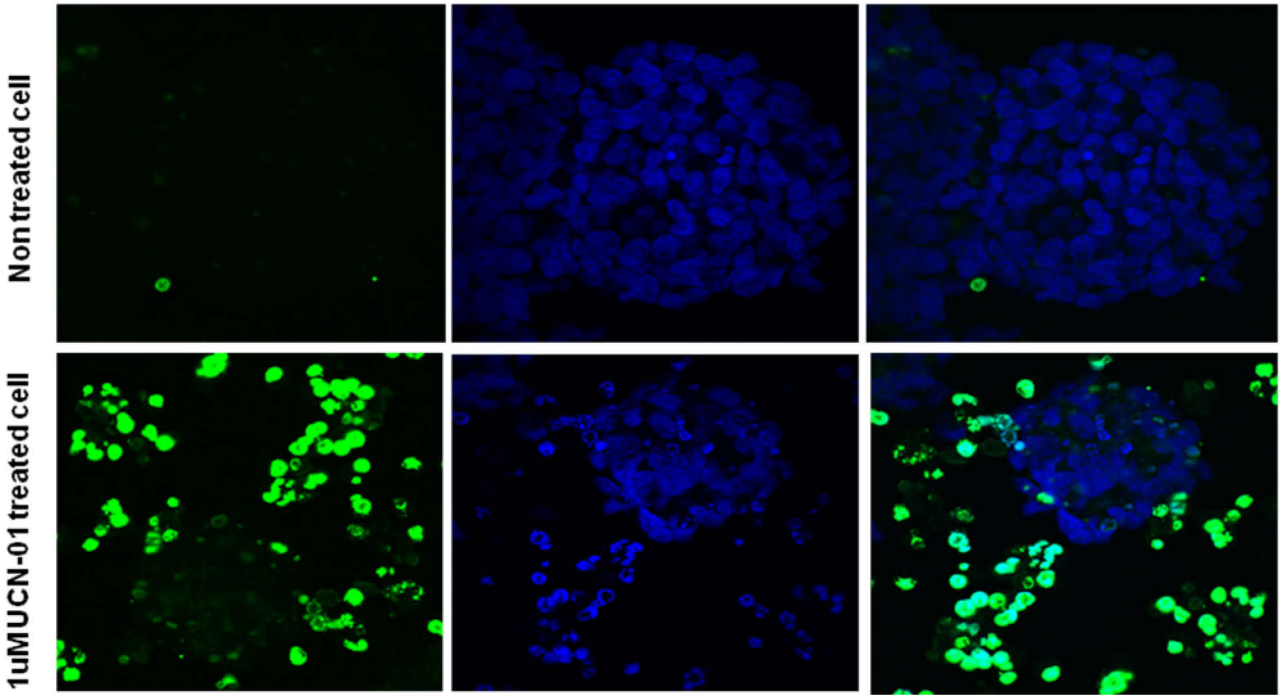

Figure 12. Immunofluorescence on tunel assayed GBM-SC line #1 treated with UCN-01 at 1 μM concentration for 96 hours. After treatment, almost 50% of cells underwent apoptosis (in green).

Effects of UCN-01 on GBM-SCs intracerebral xenografts

Intracerebral injection of human GBM-SCs in immunocompromised mice generate highly infiltrative tumor xenografts that closely mimic the behaviour of malignant gliomas (Pallini et al, 2008; Ricci-Vitiani *et al*, 2008). Within a few weeks after grafting, GBM-SCs colonize the injection site and spread towards distant brain regions with a special tropism for the large paths of white matter. These cells are particularly resistant to conventional chemotherapy drugs (Eramo *et al,* 2006). We used brain xenografts of GBM-SCs as an experimental paradigm to assess whether UCN-01 retains its anti-tumor effect in the *in vivo* condition. A stable GFP-expressing GBM-SC line, which shows the same *in vitro* proliferation and differentiation

response to UCN-01 as the parental line, was grafted into the striatum of NOD-SCID mice. By 8 weeks after grafting, control mice (*n,* 6) harboured tumors that invaded the homolateral striatum, piriform cortex, corpus callosum, anterior commissure, internal capsule, optic tract, septal nuclei, and fimbria-hyppocampus (Figure. 13A). In UCN-01 treated mice (*n,* 6), the degree of brain invasion was significantly reduced as compared to controls (Figure. 14B). The volume of the brain region invaded by GFP^+ GBM-SCs was 10.46 $\pm$ 2.03 (mean $\pm$ sd) and 0.78 $\pm$ 0.46 mm^3 in control and UCN-01 treated mice, respectively ($p<0.0001$, Student-*t* test; Figure.13C). In addition, treatment with UCN-01 dramatically lowered the density of tumor cells in the grafted striatum, which scored 129.6 $\pm$ 48.68 (mean $\pm$ sd) and 15.13 $\pm$ 19.8 cells *per* high power field in control and UCN-01 treated mice, respectively ($p<0.0001$, Student-*t* test; Figure. 13D). At the brain site where UCN-01 was injected, agglomerates of autofluorescent cell debris could be observed; however, pathological changes of the brain parenchyma, like poroencephalic cysts or glial scarring that may suggest UCN-01 toxicity, were not found.

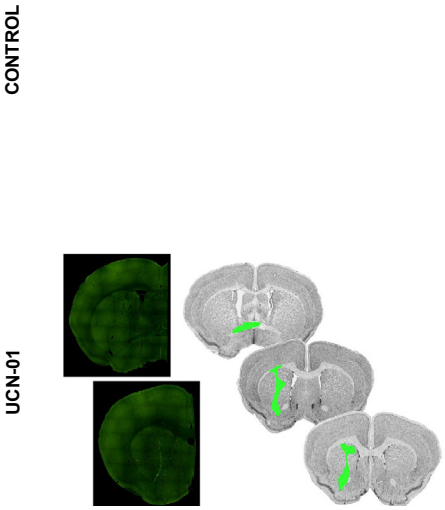

Figure 13. Effects of UCN-01 on the growth of intracerebral GBM xenografts. Mice were injected intracerebrally with GFP-expressing GBM-SCs. A)**,** By 8 weeks after grafting, control mice showed tumor cells in the homolateral striatum, piriform cortex, corpus callosum, anterior commissure, internal capsule, optic tract, septal nuclei, and fimbria-hyppocampus. *Left panel,* photomontage of 2 adjacent coronal brain sections 240 μm apart; *middle panel,* schematic drawings of 3 adjacent sections 120 μm apart showing area demarcation for calculating tumor volume; *right panel,* density of tumor cells in the grafted striatum (*upper picture)* and anterior commissure (*lower picture)*. B), Brain specimen of UCN-01 treated mouse showing inhibited growth and infiltrative potential by GBM-SCs. The brain area injected with UCN-01 showed autofluorescent cell debris without remarkable changes of the brain parenchyma (*upper right panel*). C-D)**,** Diagrams showing that both the volume of the brain region invaded by the GFP-expressing GBM-SCs and the density of these cells in the grafted striatum are significantly smaller in UCN-01 treated mice as compared with controls (**, $p<0.0001$).

Discussion

A possible explanation of cancer onset is that one or more mutations convert normal stem cells into aberrant counterparts responsible for tumor generation and propagation. According to the cancer stem cell (CSC) hypothesis, only a rare subset of cells drives tumor formation and this has major implications for the development of new therapeutic strategies aimed at targeting and eradicating the tumor stem cell population. Traditional chemotherapeutic regimens indiscriminately kill proliferating cells, thus failing to account for potential differences in drug sensitivity or target expression between CSCs and the more numerous non tumorigenic malignant cells. CSCs may well survive to treatments and relapse may then occur as the result of CSC-driven expansion. Drugs able to kill CSCs may be overlooked in screening methods that rely on rapid reduction of cell number/tumor size, while screenings specifically designed to target tumorigenic cells may yield more effective antitumor treatments. However, a systematic approach to identify and challenge the CSC survival machinery has never been undertaken, thus delaying the development of CSC targeted therapies. Latest genome-wide analyses of cancer revealed the existence of a great genetic variation among individual tumors, which makes extremely complex the use of an exclusive genomic approach to cancer biology. At the same time, it is increasingly clear that tumors share common features at the protein pathway level, suggesting that a pathway-oriented perspective would represent the most effective approach to drug discovery and therapy.

Glioblastoma multiforme (GBM) is the most common brain tumor in adults and is nearly uniformly fatal. Advances in neuroimaging, microsurgical techniques and radio- and chemotherapy protocols have not significantly lengthened the survival of GBM patients. The recent demonstration that human GBMs contain tumorigenic neural stem-like cells indicate that neural stem and/or progenitor cells are a plausible origin for human gliomas, leading to the speculation that more effective therapies will result from approaches aimed at targeting the stem cell-like component of GBM.

In this thesis project we have exploited two strategies aimed at elucidating the molecular pathways that sustain the survival and proliferation of the stem cell compartment within GBM: the first is a microRNA (miRNA) expression profiling in GBM-SCs in order to find a miRNA-based therapy and the second is a proteomic profiling in order to find compounds that specifically target GBM-SCs survival pathways.

MicroRNAs (miRNAs), a wide class of small, noncoding RNAs that negatively regulate protein expression at the post-transcriptional level, are emerging as important regulators of cellular differentiation and proliferation and players in the etiology and progression of a variety of cancers.

Starting from the observation that the expression profile of miRNAs can be used to classify a tissue and its pathology, in some case with more precision than using other subsets of genes, several studies have demonstrated that the miRNAs could represent ideal therapeutic targets because of their involvement in biological processes that are aberrant in cancer. Indeed, growing evidence suggests that the alteration of miRNA levels can have a causative role in disease development. The issue of miRNA-based therapy is gaining growing interest in the scientific community, as it is established that restoring normal expression levels of selected miRNAs in tumors results in a dramatic anti-neoplastic effect. Although the understanding of the miRNA role in cancer is still partial, their therapeutic application is being pursued by two possibile approaches: blocking oncogenic miRNAs or over-expressing miRNAs with tumor suppressor activity. Elucidation of the molecular players involved in differentiation pathways which are aberrant in GBM-SCs is critical to better understand the pathogenesis of brain tumors. Furthermore, through intercrossing with miRNA target analyses, and compound library screening, we have identified molecular target potentially responsible for the survival and tumorigenicity of GBM-SCs.

Deregulation of gene expression is currently one of the most actively investigated features of diseased tissue, both for diagnostic and therapeutic purposes. The identification of recurrent patterns of differential gene expression between normal and diseased tissue has helped to clarify that gene profiles are intertwined with the array of mutation that are causative to the genesis of a given pathology. Some of the most known oncogenic lesions, for example those leading to loss of function of TP53 or to c-Myc overexpression, have been found to entail the differential expression of a subset of miRNAs that, might be an active player in the mechanism of oncogenesis/oncosuppression, hence representing a possible point of therapeutic intervention.

To distinguish between miRNAs whose downregulation is a mere bystander event to the oncogenic lesion, and those which are intrinsic to oncosuppression, functional assays can be performed, where their transcript are reexpressed back to normal levels. We found that enhanced expression of miR-135b in GBM-SCs might lead to oncosuppression by altering the

cells ability to proliferate, migrate and grow in an anchorage independent manner. Coherent with these observations, we have tested the effect of miR-135b in *in vivo* model , our experiments of *in vivo* trasplantation into the brain of NOD/SCID mice showed that enhanced expression of miR-135b provokes a sensible delay of brain invasion of infected cells. The definition of the subset of miRNA target genes that mediate an oncosuppressor/oncogenic effect is one of the most intriguing aspects of this field of study, as it is probably the element that by itself can explain most of the mechanism of action which eventually needs to be tackled by a therapeutic instrument. Reports abound where a single miRNA-target gene interaction is claimed to be responsible for a given effect, although search engines typically return hundreds of target transcripts to a single miRNA query. In our study, to understand more deeply the mechanism by which this miRNA can behave as oncosuppressor, we will try to establish whether any of its putative targets represent a crucial function in GBM progression.

First we will select, among the target genes predicted by TargetScan, transcripts which are particularly relevant for their putative role in GBM progression. Next, we will analyze the levels of target proteins at different time points after the induction of the transgene in cells transduced with either pTRIPZred or pTRIPZred-135b, coupled with the monitoring of transcript levels for both the induced miRNA and target transcripts. Then, we will investigate whether the decrease in the target proteins is attributed to the direct action of the overexpressed miR-135b on target transcripts. To do this aim, in the future we will perform a luciferase-reporter assay by cloning individual targeted regions as 3'UTR after the reporter protein coding sequence. MiRNAs have emerged as key players in posttranscriptional gene regulation, and as indispensable mediators of several important biological processes, including tumorigenesis and tissue homeostasis and regeneration. In their unique biochemical nature lies a great advantage over protein-encoding genes: it is becoming evident that, if a gene therapy would be required, miRNA synthesis, stability, and delivery to target cells is much more feasible and immediate than for proteins. It has recently been shown that the use of an adeno-associated virus for restoration of a miRNA in a murine model of hepatocellular carcinoma has a tremendous impact on tumor progression. Besides viral-based therapy, other studies support the possibility that miRNAs can be delivered systemically to target organs, without the risk of immune reaction. This prompts for extensive investigation of the potential role of miRNAs in GBM and as instruments of molecular therapy. For the second strategy, in this thesis, we performed an RPPA analysis on several GBM-SC lines. Results showed a great molecular heterogeneity

among different patients, thus hindering the identification of a single common potential therapeutic target. Therefore, using a reverse approach, GBM-SC lines were subsequently subjected to an *in vitro* screening of 80 protein kinase inhibitors with known targets and mechanisms of action. This analysis led to the identification of several pathways crucially involved in proliferation and survival of GBM-SCs such as EGFR, VEGFR and their downstream pathways PI3K/AKT (AKT, GSK3, mTOR, PKC) and Ras (MEK, p38MAPK, p70S6K). Although preliminary data suggested that there is not clear correlations between specific activated pathways and GBM subtype, in line with the extreme heterogeneity of this tumor, we have evaluated the possibility to overcome chemoresistance of GBM-SCs by treatment with specific inhibitors of those survival pathways. Our results indicated that UCN-01 has a cytotoxic effect on several GBM-SC lines. UCN-01 is a Staurosporine derivative initially identified as a PKC inhibitor that is also able to inhibit PDK1 (3-phosphoinositide-dependent kinase 1) and Chk1 (Checkpoint Kinase 1) kinase. This compound is currently used as antineoplastic agent, in combination with chemotherapy, in phase I clinical trials for solid tumors treatment (Fracasso, et al.,2010 , Kummar, et al.,2010 and Hotte, et al.,2006). All GBM-SCs lines were *in vitro* sensitive to UCN-01 that targets the PKC and Chk1 pathways. UCN-01 effects on PKC inhibition, and in particular on PKCβII isoforms, was based on a reduction of these protein autophosphorylation processes (threonine 638 and 641), which are necessary for catalytic activity maintenance (Bornancin, and Parker ., 1996 and Newton ., et al 1995). PKCα isoform is known to exert its function as a promoter of cell survival by modulating the expression or the activity of antiapoptotic proteins Bcl-2 and Bcl-XL (Anderson, et al., 2003 and Hsieh, et al 2003). The ability of UCN-01 to inhibits GBM-SCs growth could also, at least in part, be attributed to Chk1 kinase inhibition, as demonstrated by the reduced levels of phosphorylation of the Chk1 target, cdc25 phosphatase. In response to spontaneous DNA damage, Chk1 phosphorylates cdc25 thus preventing cell cycle advancement, these could be another mechanism through which UCN-01 exerts its effect. UCN-01 posses a much higher activity and a much lower toxicity than Staurosporine, however its ability to interfere with various protein kinases activity (PKC, Chk1) could be the real basis for its effects.

Therefore a better molecular characterization of UCN-01 molecular mechanism of action, in order to understand the relative weight of these processes, will be of major interest.

The purpose of this project was the molecular characterization of GBM-SC survival pathways through an integrated strategy that incorporates information obtained from i) miRNA signatures; ii) drug screening. This project has proposed an innovative interpretation of tumor development which will be studied with up to date methodological approaches. Its results could contribute to develop new therapies to block the progression of a highly lethal disease such as GBM and could also promote a similar evaluation in other malignancies and have a more general impact in oncology.

References

Taphoorn et al., *Health-related quality of life in patients with glioblastoma :a randomised controlled trial.* Lancet Oncol.2005 Dec;6(12) :937-44

A.F.Carpentier and J.Y. Delattre et al ., *EGFR-tyrosine kinase domain mutations in human gliomas.* Neurology.2005 April 26;64(8):1444-5

Hirschmann-Jax, C. et al. *A distinct "side population" of cells with high drug efflux capacity in human tumor cells.* Proc Natl Acad Sci *U S A*(2004) 101, 14228-33.

Dean, M., Fojo, T. & Bates, S. *Tumour stem cells and drug resistance*. Nat Rev Cancer(2005) 5, 275-84.

Miller CR, Perry A. *Glioblastoma.* Arch. Pathol Lab. Med. 2007 Mar;131(3):397-406. Review.

Frank B et al ., *Enzastaurin-induced apoptosis in glioma cells is caspase-dependent and inhibited by BCL-XL.* j. Neurochem 2008 Sep;106(6):2436-48.

Curado MP, Edwards B, Shin HR, et al, editors. *Cancer incidence in five continents, volume IX.* Lyon, France: IARC Scientific Publications No. 160; 2007.

Fisher JL, Schwartzbaum JA, Wrensch M, Wiemels JL. *Epidemiology of brain tumors*. Neurol Clin. 2007 Nov;25(4):867,90,

Bondy ML, Scheurer ME, Malmer B, Barnholtz-Sloan JS, Davis FG, Il'yasova D, et al. *Brain tumor epidemiology: Consensus from the brain tumor epidemiology consortium*. Cancer. 2008 Oct 1;113(7 Suppl):1953-68.

Wrensch M, Minn Y, Chew T, Bondy M, Berger MS. *Epidemiology of primary brain tumors: Current concepts and review of the literature.* Neuro Oncol. 2002 Oct;4(4):278-99.

Louis DN, Ohgaki H, Wiestler OD, Cavenee WK. *WHO classification of tumours of the central nervous system*. 4th ed. Louis DN, Ohgaki H, Wiestler OD, Cavenee WK, editors. Lyon, France: International Agency for Research on Cancer (IARC); 2007.

Ohgaki H, Kleihues P. *Genetic pathways to primary and secondary glioblastoma*. Am J Pathol. 2007 May;170(5):1445-53.

Furnari FB, Fenton T, Bachoo RM, Mukasa A, Stommel JM, Stegh A, et al. *Malignant astrocytic gli-oma: Genetics, biology, and paths to treatment*. Genes Dev. 2007 Nov 1;21(21):2683-710.

Das S, Srikanth M, Kessler JA. *Cancer stem cells and glioma*. Nat Clin Pract Neurol. 2008 Aug;4(8):427-35.

Stiles CD, Rowitch DH. *Glioma stem cells: A midterm exam.* Neuron. 2008 Jun 26;58(6):832-46.

Verstappen, J., et al., *A functional model for adult stem cells in epithelial tissues.* Wound Repair Regen, 2009. 17(3): p. 296-305.

Becker, A.J., C.E. Mc, and J.E. Till, *Cytological demonstration of the clonal nature of spleen colonies derived from transplanted mouse marrow cells.* Nature, 1963. 197: p. 452-4.

Furth, J. and M.C. Kahn, *The transmission of leukaemia of mice with a single cell.* Am J. Cancer, 1937. 31: p. 276–282.

Heppner, G.H., *Tumor heterogeneity.* Cancer Res, 1984. 44(6): p. 2259-65.

Hamburger, A. and S.E. Salmon, *Primary bioassay of human myeloma stem cells.* J Clin Invest, 1977. 60(4): p. 846-54.

Reya, T., et al., *Stem cells, cancer, and cancer stem cells.* Nature, 2001. 414(6859): p. 105-11.

Bonnet, D. and J.E. Dick, *Human acute myeloid leukemia is organized as a hierarchy that originates from a primitive hematopoietic cell.* Nat Med, 1997. 3(7): p. 730-7.

Baum, C.M., et al., *Isolation of a candidate human hematopoietic stem-cell population.* Proc Natl Acad Sci U S A, 1992. 89(7): p. 2804-8.

Osawa, M., et al., *Long-term lymphohematopoietic reconstitution by a single CD34-low/negative hematopoietic stem cell.* Science, 1996. 273(5272): p. 242-5.

Lininger, R.A., et al., *Comparison of loss heterozygosity in primary and recurrent ductal carcinoma in situ of the breast.* Mod Pathol, 1998. 11(12): p. 1151-9.

Goodell, M.A., et al., *Isolation and functional properties of murine hematopoietic stem cells that are replicating in vivo.* J Exp Med, 1996. 183(4): p. 1797-806.

Kondo, T., T. Setoguchi, and T. Taga, *Persistence of a small subpopulation of cancer stem-like cells in the C6 glioma cell line.* Proc Natl Acad Sci U S A, 2004. 101(3): p. 781-6.

Hirschmann-Jax, C., et al., *A distinct "side population" of cells with high drug efflux capacity in human tumor cells.* Proc Natl Acad Sci U S A, 2004. 101(39): p. 14228-33.

Nakai, E., et al., *Enhanced MDR1 expression and chemoresistance of cancer stem cells derived from glioblastoma.* Cancer Invest, 2009. 27(9): p. 901-8.

Shervington, A. and C. Lu, *Expression of multidrug resistance genes in normal and cancer stem cells.* Cancer Invest, 2008. 26(5): p. 535-42.

Liu, G., et al., *Analysis of gene expression and chemoresistance of CD133+ cancer stem cells in glioblastoma.* Mol Cancer, 2006. 5: p. 67.

Bao, S., et al., *Glioma stem cells promote radioresistance by preferential activation of the DNA damage response.* Nature, 2006. 444(7120): p. 756-60.

Ricci-Vitiani, L., et al., *Colon cancer stem cells.* J Mol Med, 2009. 87(11): p. 1097-104.

Singh SK, Clarke ID, Terasaki M, et al. Identification of a cancer stem cell in human brain tumors. Cancer Res 2003*;*63*:*5821*–8.*

Singh SK, Hawkins C, Clarke ID, et al. Identification of human brain tumour initiating cells. Nature 2004;432:396–401

Ogden AT, Waziri AE, Lochhead RA, et al. Identification of A2B5^{+}CD133^{-} tumor-initiating cells in adult human gliomas. Neurosurgery 2008*;*62*:*505*–14; discussion 514–505.*

Wu A, Oh S, Wiesner SM, et al. Persistence of CD133^{+} cells in human and mouse glioma cell lines: detailed characterization of GL261 glioma cells with cancer stem cell-like properties. Stem Cells Dev 2008;17:173–84.
Liu G, Yuan X, Zeng Z, et al. Analysis of gene expression and chemoresistance of CD133^{+} cancer stem cells in glioblastoma. Mol Cancer 2006*;*5*:*67.

Bao S, Wu Q, McLendon RE, et al. Glioma stem cells promote radioresistance by preferential activation of the DNA damage response. Nature 2006

Gunther HS, Schmidt NO, Phillips HS, et al. Glioblastoma-derived stem cell-enriched cultures form distinct subgroups according to molecular and phenotypic criteria. Oncogene *2008;27:2897–909*

Zeppernick F, Ahmadi R, Campos B, et al. Stem cell marker CD133 affects clinical outcome in glioma patients. Clin Cancer Res 2008*;*14*:*123*–9.*

Ambros V, Lee RC. *Identification of microRNAs and other tiny noncoding RNAs by cDNA cloning.* Methods Mol Biol. 2004;265:131-58.

Johnston RJ, Hobert O . *A microRNA controlling left/right neuronal asymmetry in Caenorhabditis elegans.* Nature 2003; 426:845-849.

Ambros V., et al. *The C. elegans heterochronic gene lin-4 encodes small RNAs with antisense complementary to lin-14.*Cell 75:843-854.

Hannon GJ., et al ., *Dicer is essential for mouse development*. Nat.Genet 35:215-217.

Chen CZ, Li L, Lodish HF, Bertel DP. *MicroRNAs modulate hematopoietic lineage differentiation.* Science 303:83-86.

Miska EA. How microRNAs control cell division differentiation and death. Curr.Opin.Genet.Dev 15:563-568.

Miska EA., et al. *Microarray analysis of microRNA expression in the developing mammalian brain.* Genome Biol 5:R68.

Lu J, et al . *MicroRNA expression profiles classify human cancers.* Nature 435:834-838.

Calin GA, Sevignani C, Dumitru CD, Hyslop T, Noch E, Yendamuri S, Shimizu M, Rattan S, Bullrich F, NegriniM, Croce CM. *Human microRNA genes are frequently located at fragile sites and genomic regions involved in cancers.*. Proc Natl Acad Sci U S A. 2004 Mar 2;101(9):2999-3004

Ciafrè SA, Galardi S, Mangiola A, Ferracin M, Liu CG, Sabatino G, Negrini M, Maira G, Croce CM, Farace MG. *Extensive modulation of a set of microRNAs in primary glioblastoma.* Biochem Biophys Res Commun. 2005 Sep 9;334(4):1351-8.

Chen CZ. *MicroRNAs as oncogenes and tumor suppressors.* N Engl J Med. 2005 Oct 27;353(17):1768-71

Kefas B, Godlewski J, Comeau L, Li Y, Abounader R, Hawkinson M, Lee J, Fine H, Chiocca EA, Lawler S, Purow B.*MicroRNA-7 inhibits the epidermal growth factor receptor and the Akt pathway and is down-regulated in glioblastoma*. Cancer Res. 2008 May 15;68(10):3566-72

Calin GA, Croce CM , et al. *A microRNA expression signature of human solid tumors defines cancer gene targets*. Proc Natl Acad Sci U S A. 2006 Feb 14;103(7):2257-61. Epub 2006 Feb 3.

Zhu S, Wu H, Wu F, Nie D, Sheng S, Mo YY. *MicroRNA-21 targets tumor suppressor genes in invasion and metastasis.* Cell Res. 2008 Mar;18(3):350-9

Gabriely G, Wurdinger T, Kesari S, Esau CC, Burchard J, Linsley PS, Krichevsky AM. *MicroRNA 21 promotes glioma invasion by targeting matrix metalloproteinase regulators*. Mol Cell Biol. 2008 Sep;28(17):5369-80. Epub 2008 Jun 30.

Godlewski J, Nowicki MO, Bronisz A, Williams S, Otsuki A, Nuovo G, Raychaudhury A, Newton HB, Chiocca EA, Lawler S. *Targeting of the Bmi-1 oncogene/stem cell renewal factor by microRNA-128 inhibits glioma proliferation and self-renewal.*Cancer Res. 2008 Nov 15;68(22):9125-30.

Silber J, Lim DA, Petritsch C, Persson AI, Maunakea AK, Yu M, Vandenberg SR, Ginzinger DG, James CD, Costello JF, Bergers G, Weiss WA, Alvarez-Buylla A, Hodgson JG. miR-124 *and* miR-137 *inhibit proliferation of glioblastoma multiforme* cells *and induce differentiation of brain tumor* stem cells. BMC Med. 2008 Jun 24;6:14.

Gal H,et al. *MIR-451 and Imatinib mesylate inhibit tumor growth of Glioblastoma stem cells*.Biochem Biophys Res Commun. 2008 Nov 7;376(1):86-90. Epub 2008 Aug 31.

Shi L, Cheng Z, Zhang J, Li R, Zhao P, Fu Z, You Y. *hsa*-mir-*181a and hsa*-mir-*181b function as tumor suppressors in human glioma cells.* Brain Res. 2008 Oct 21;1236:185-93. Epub 2008 Jul 30.

Spurrier, B., et al., *Protein and lysate array technologies in cancer research.* Biotechnol Adv, 2008. 26(4): p. 361-9.
Spurrier, B., S. Ramalingam, and S. Nishizuka, *Reverse-phase protein lysate microarrays for cell signaling analysis.* Nat Protoc, 2008. 3(11): p. 1796-808.

Figg WD.,et al. *Review of UCN-01 development: a lesson in the importance of clinical pharmacology.* J Clin Pharmacol. 2005 Apr;45(4):394-403. Review.

Akinaga et al. *Antitumor activity of UCN-01, a selective inhibitor of protein kinase C, in murine and human tumor models.* Cancer Res. 1991 Sep 15;51(18):4888-92

Seynaeve CM, Stetler-Stevenson M, Sebers S, Kaur G, Sausville EA, Worland PJ .*Cell cycle arrest and growth inhibition by the protein kinase antagonist* UCN-01 *in human breast carcinoma cells.* Cancer Res. 1993 May 1;53(9):2081-6.

Busby EC, Leistritz DF, Abraham RT, Karnitz LM, Sarkaria JN.*The radiosensitizing agent* 7-hydroxystaurosporine *(*UCN-01*) inhibits the DNA damage checkpoint kinase hChk1.* Cancer Res. 2000 Apr 15;60(8):2108-12.

Yu Q, La Rose J, Zhang H, Takemura H, Kohn KW, Pommier Y.*UCN-01 inhibits p53 up-regulation and abrogates gamma-radiation-induced G(2)-M checkpoint independently of p53 by targeting both of the checkpoint kinases, Chk2 and Chk1*. Cancer Res. 2002 Oct 15;62(20):5743-8.

Graves PR, Yu L, Schwarz JK, Gales J, Sausville EA, O'Connor PM, Piwnica-Worms H. *The Chk1 protein kinase and the Cdc25C regulatory pathways are targets of the anticancer agent UCN-01*. J Biol Chem. 2000 Feb 25;275(8):5600-5.

Sato S, Fujita N, Tsuruo T. *Interference with PDK1-Akt survival signaling pathway by UCN-01 (7-hydroxystaurosporine).*Oncogene. 2002 Mar 7;21(11):1727-38

Bunch RT, Eastman A .7-Hydroxystaurosporine (UCN-01) causes redistribution of proliferating cell nuclear antigen and abrogates cisplatin-induced S-phase arrest in Chinese hamster ovary cells. Cell Growth Differ. 1997 Jul;8(7):779-88.

Shao RG, Cao CX, Shimizu T, O'Connor PM, Kohn KW, Pommier Y. *Abrogation of an S-phase checkpoint and potentiation of camptothecin cytotoxicity by 7-hydroxystaurosporine (UCN-01) in human cancer cell lines, possibly influenced by p53 function.* Cancer Res. 1997 Sep 15;57(18):4029-35

Akiyama T, Yoshida T, Tsujita T, Shimizu M, Mizukami T, Okabe M, Akinaga S. *G1 phase accumulation induced by* UCN-01 *is associated with dephosphorylation of Rb and CDK2 proteins as well as induction of CDK inhibitor p21/Cip1/WAF1/Sdi1 in p53-mutated human epidermoid carcinoma A431 cells.* Cancer Res. 1997 Apr 15;57(8):1495-501.

Chen X, Lowe M, Keyomarsi K. *UCN-01-mediated G1 arrest in normal but not tumor breast cells is pRb-dependent and p53-independent.* Oncogene. 1999 Oct 7;18(41):5691-702

Hirose Y, Berger MS, Pieper RO. *Abrogation of the Chk1-mediated G(2) checkpoint pathway potentiates temozolomide-induced toxicity in a p53-independent manner in human glioblastoma cells.* Cancer Res. 2001 Aug 1;61(15):5843-9.

Monga M, Sausville EA. *Developmental therapeutics program at the NCI: molecular target and drug discovery process.* Leukemia. 2002 Apr;16(4):520-6.

Das N, Chattoraj DK. *Origin pairing ('handcuffing') and unpairing in the control of P1 plasmid replication.* Mol Microbiol. 2004 Nov;54(3):836-49

Chuang YY, Tran NL, Rusk N, Nakada M, Berens ME, Symons M. *Role of synaptojanin 2 in glioma cell migration and invasion.* Cancer Res. 2004 Nov 15;64(22):8271-5

Soroceanu L, Manning TJ Jr, Sontheimer H. *Modulation of glioma cell migration and invasion using Cl(-) and K(+) ion channel blockers.* J Neurosci. 1999 Jul 15;19(14):5942-54.

Tan LP, Seinen E, Duns G, de Jong D, Sibon OC, Poppema S, Kroesen BJ, Kok K, van den Berg A. *A high throughput experimental approach to identify miRNA targets in human cells.* Nucleic Acids Res. 2009 Nov;37(20):e137. Epub 2009 Sep 4.

Pallini R, Sorrentino A, Pierconti F, Maggiano N, Faggi R, Montano M, *et al. Telomerase inhibition by stable RNA interference impairs tumor growth and angiogenesis in glioblastoma xenografts.* International Journal of Cancer 2006; 118: 2158-2167.

Ricci-Vitiani L, Pallini R, Larocca LM, Lombardi DG, Signore M, Pierconti F, Petrucci G, Montano N, Maira G, De Maria R. *Mesenchymal differentiation of glioblastoma stem cells.* Cell Death Diff 2008**,** 15**(**9**):**1491-1498

Pallini R, Ricci-Vitiani L, Banna GL, Signore M, Lombardi D, Todaro M, Stassi G, Martini M, Maira G, Larocca LM, and De Maria R. *Cancer stem cell analysis and clinical outcome in patients with glioblastoma multiforme.* Clin Cancer Res, 2008; 14(24):8205-8212.

Eramo A, Ricci-Vitiani L, Zeuner A, Pallini R, Lotti F, Sette G, Pilozzi E, Larocca LM, Peschle C, De Maria R. *Chemotherapy resistance of glioblastoma stem cells.* Cell Death Diff, 2006, Jul;13(7):1238-41

Fracasso, P.M., et al., *A Phase 1 study of UCN-01 in combination with irinotecan in patients with resistant solid tumor malignancies.* Cancer Chemother Pharmacol, 2010.

Kummar, S., et al., *A phase I trial of UCN-01 and prednisone in patients with refractory solid tumors and lymphomas.* Cancer Chemother Pharmacol, 2010. 65(2): p. 383-9.

Hotte, S.J., et al., *Phase I trial of UCN-01 in combination with topotecan in patients with advanced solid cancers: a Princess Margaret Hospital Phase II Consortium study.* Ann Oncol, 2006. 17(2):
p. 334-40.

Gutcher, I., P.R. Webb, and N.G. Anderson, *The isoform-specific regulation of apoptosis by protein kinase C.* Cell Mol Life Sci, 2003. 60(6): p. 1061-70.

Hsieh, Y.C., et al., *Suppression of protein kinase Calpha triggers apoptosis through down-regulation of Bcl-xL in a rat hepatic epithelial cell line.* Shock, 2003. 19(6): p. 582-7.

Bornancin, F. and P.J. Parker, *Phosphorylation of threonine 638 critically controls the dephosphorylation and inactivation of protein kinase Calpha.* Curr Biol, 1996. 6(9): p. 1114-23.

Keranen, L.M., E.M. Dutil, and A.C. Newton, *Protein kinase C is regulated in vivo by three functionally distinct phosphorylations.* Curr Biol, 1995. 5(12): p. 1394-1403.